

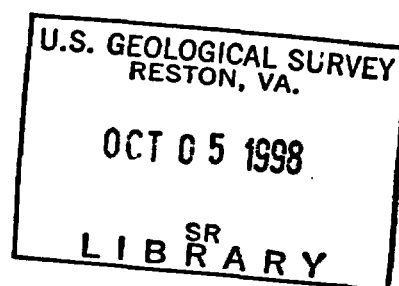
(230)
R290
No. 98-83
==

APPLICATIONS OF ISOTOPE GEOCHEMISTRY TO THE RECONSTRUCTION OF YUCCA MOUNTAIN, NEVADA, PALEOHYDROLOGY—STATUS OF INVESTIGATIONS: JUNE 1996

U.S. GEOLOGICAL SURVEY

Open-File Report 98-83

Prepared in cooperation with the
NEVADA OPERATIONS OFFICE,
U.S. DEPARTMENT OF ENERGY, under
Interagency Agreement DE-AI08-97NV12033



Applications of Isotope Geochemistry to the Reconstruction of Yucca Mountain, Nevada, Paleohydrology—Status of Investigations: June 1996

**By Joseph F. Whelan, Richard J. Moscati, Sarah B.M. Allerton, and
Brian D. Marshall**

U.S. GEOLOGICAL SURVEY

Open-File Report 98-83

**Prepared in cooperation with the
NEVADA OPERATIONS OFFICE,
U.S. DEPARTMENT OF ENERGY, under
Interagency Agreement DE-AI08-97NV12033**

**Denver, Colorado
1998**

**U.S. DEPARTMENT OF THE INTERIOR
BRUCE BABBITT, Secretary**

**U.S. GEOLOGICAL SURVEY
Thomas J. Casadevall, Acting Director**

The use of firm, trade, and brand names in this report is for identification purposes only and does not constitute endorsement by the U.S. Geological Survey.

For additional information write to:

**District Chief
U.S. Geological Survey
Box 25046, Mail Stop 415
Denver Federal Center
Denver, CO 80225-0046**

**Copies of this report can be purchased
from:**

**U.S. Geological Survey
Information Services
Box 25286
Federal Center
Denver, CO 80225**

CONTENTS

Abstract.....	1
Introduction.....	1
Sample Distribution	3
Sampling and analytical methods	3
Paragenesis of Exploratory Studies Facility Occurrences	6
Most recent event: Calcite or opal? - Precipitation or dissolution?	8
Dissolution events within the unsaturated zone?	8
Isotopic Data	13
Implications of new Exploratory Studies Facility data to previous interpretations	13
Carbon-13-enriched calcite from the Exploratory Studies Facility	13
Silica-phase oxygen isotope studies	15
Radiocarbon geochronologic studies	18
Conclusions.....	21
References Cited	21
Appendixes	23

FIGURES

1. Maps showing location of the Yucca Mountain region, Nevada, the potential repository site, the Bullfrog Mine, sampled boreholes, Trench 14, and the Exploratory Studies Facility.....	4
2. Map showing location of the Exploratory Studies Facility, topographic features, prominent faults, and the locations of sampled secondary mineralization occurrences near Yucca Mountain, Nevada	5
3. Schematic illustrations of the typical paragenetic sequences found (a) in lithophysal cavities and (b) on fracture surfaces	7
4a.-4h. Photomicrographs showing:	
4a. Late botryoidal opal with rhombic overgrowths of calcite that are, in turn, locally pimpled with tiny opaline spheres	9
4b. Late botryoidal opal grown on calcite and partially engulfed by a later stage of calcite.....	9
4c. Opal with overgrowths of a later opaline stage followed by calcite overgrowth coated with botryoidal opal that is, in turn, partially buried by late calcite	10
4d. Bladed calcite crystals with scepter-like terminations	10
4e. Pyramidal to spire-like calcite forms from the basal zone of lithophysal secondary calcite mineralization	11
4f. Basal dissolution zone, with calcite microspeleothems or meniscus cements.....	11
4g. Unetched surface of calcite crystal	12
4h. Pitted surface of apparently etched calcite crystal face	12
5-7. Graphs showing:	
5. Distribution of unsaturated-zone delta carbon-13 and delta oxygen-18 values of calcite plotted against depth	14
6. Distribution of delta carbon-13 and delta oxygen-18 values of Exploratory Studies Facility calcite samples plotted against distance from the portal.....	14
7. Preliminary radiogenic strontium isotopic compositions plotted against the stable carbon and oxygen isotopic compositions, and correlation of delta carbon-13 and delta oxygen-18 values of Exploratory Studies Facility calcite.....	16
8-9. Histograms showing:	
8. Yucca Mountainun unsaturated zone secondary silica delta oxygen-18 values.....	17
9. Distribution of carbon-14 ages from Exploratory Studies Facility calcite occurrences	20

TABLE

1. Major stratigraphic units in the Late Cenozoic volcanic rock sequence of the Yucca Mountain area, Nevada..... 3

Multiply	By	To obtain
centimeter (cm)	0.3937	inch
meter (m)	3.2808	foot
kilometer (km)	0.6214	mile

Degree Celsius (°C) may be converted to degree Fahrenheit (°F) by using the following equation:

$$^{\circ}\text{F} = 9/5 (^{\circ}\text{C}) + 32$$

Sea level: In this report "sea level" refers to the National Geodetic Vertical Datum of 1929 (NGVD of 1929)—a geodetic datum derived from a general adjustment of the first-order level nets of both the United States and Canada, formerly called Sea Level Datum of 1929.

The following terms also are used in this report:

Ma	millions of years old
Ka	thousands of years old
Ky	thousands of years
Pz	Paleozoic
ESF	Exploratory Studies Facility
SMOW	Standard Mean Ocean Water
PDB	Pee Dee Belemnite
°C/km	degrees Celsius per kilometer
AMS	Accelerator Mass Spectrometer
pmc	percent modern carbon
N	normal

Applications of Isotope Geochemistry to the Reconstruction of Yucca Mountain, Nevada, Paleohydrology—Status of Investigations: June 1996

By Joseph F. Whelan, Richard J. Moscati, Sarah B.M. Allerton, and Brian D. Marshall

Abstract

Tunneling of the Exploratory Studies Facility has offered the opportunity to sample and examine occurrences of secondary mineralization found in the unsaturated-zone tuffs of Yucca Mountain, Nevada. Petrographic and paragenetic analyses, calcite and silica-phase stable isotopic analyses, and preliminary strontium tracer isotope and radiocarbon age analyses of these samples indicate that (1) an early stage of secondary mineralization consisting largely of chalcedony and quartz, but possibly with or slightly preceded by calcite, probably formed at warmer than ambient temperatures; (2) later secondary mineralization consisting of calcite and opal appears completely consistent with formation from percolation of surface infiltration whose solute load and carbon isotopic compositions reflect passage through the overlying soils; (3) based on textural studies, all unsaturated-zone secondary mineral occurrences exposed within the Exploratory Studies Facility tunnel, with the exception of the vapor-phase assemblages that formed at high temperatures during cooling of the tuffs, probably formed in unsaturated settings; and (4) calcite radiocarbon ages, based on preliminary results, have not been compromised by post-depositional exchange with carbon-bearing water and gases in the unsaturated zone.

INTRODUCTION

Yucca Mountain, Nevada, is presently under evaluation as a potential national subsurface repository for high-level radioactive wastes. Current designs for the potential repository would emplace wastes within the sequence of welded and nonwelded tuffs in the thick unsaturated zone of the mountain, several hundred meters below ground surface but still well above the modern water table. Siting within the unsaturated zone is advantageous in that it isolates the wastes from regional ground water; unfortunately, it also introduces climate-driven infiltration and percolation through the unsaturated zone as site-evaluation variables. Although present climate is arid, past climates have ranged to much wetter (R.M. Forester, U.S. Geological Survey, oral commun., 1997), and future climates are likely to be wetter, as well. The effects of future climatic changes on site performance are critical issues for site suitability assessment.

Efforts to reconstruct the hydrologic response of Yucca Mountain to past climatic variations, especially within the unsaturated zone, have focused on textural and geochemical study of secondary minerals deposited from past percolation fluxes and ground water. This report discusses stable carbon and oxygen isotopic data and mineral parageneses determined from secondary calcite and silica mineralization and describes reconnaissance radiogenic strontium (Sr) isotopic and carbon-14 (^{14}C) age data and their applicability to paleohydrologic and paleoclimatic studies. Most of the new data reported here were collected from samples of secondary mineral occurrences accessed during construction of the Exploratory Studies Facility (ESF) tunnel. Construction of the tunnel was a fundamental component of site-characterization studies of Yucca Mountain.

Evolution of understanding of the origins of secondary minerals within the Yucca Mountain tuffs is reflected in several papers (Whelan and Stuckless, 1990 and 1992; Whelan and others, 1994; and J.F. Whelan and R.J. Moscati, U.S. Geological Survey, written commun., 1997). The latter report summarized the evolution of studies of the secondary calcite and silica minerals within Yucca Mountain and updated understanding of the processes responsible for deposition of these minerals. It stated that:

"investigation of the secondary minerals within the mountain, spurred by the study of the surficial deposits, revealed that the calcite and opal commonly coating fractures and lining open cavities in the unsaturated zone were deposited during downward percolation of meteoric waters ... These fluids reflected the oxygen isotopic signature of precipitation ... and had acquired distinctive carbon and strontium isotopic signatures from the thin overlying soils during infiltration that were recorded by the secondary calcite and opal deposited by the fluids as they percolated through the tuffs." (Emphasis added.)

A stage of the secondary calcite, paragenetically early but volumetrically minor, is characterized by uncommonly carbon-13 (^{13}C)-enriched isotopic compositions and by delta oxygen-18 ($\delta^{18}\text{O}$) values that decrease more rapidly with depth than succeeding calcite stages. That steeper $\delta^{18}\text{O}$ decrease may record a steeper geothermal gradient during formation of the paragenetically early calcite. Data collected from ESF occurrences during 1996 indicate that, at least locally, this paragenetically early calcite is volumetrically more abundant than drill hole studies had indicated.

Other studies of secondary mineralization in the ESF estimated Pleistocene percolation fluxes through the unsaturated zone by measuring secondary calcite and opal volumes and inferring rates of secondary calcite and opal formation from thorium-230/uranium ($^{230}\text{Th}/\text{U}$) and ^{14}C age determinations. If that early calcite stage were formed much earlier and under significantly different hydrologic conditions, as is suggested by its atypical $\delta^{13}\text{C}$ systematics, then its inclusion in the mineral record used to estimate past percolation fluxes might result in erroneous flux estimates.

This report describes efforts to map the parageneses of secondary mineral occurrences (appendix 1) within the ESF, discusses the stable carbon and oxygen isotopic compositions of calcite, the stable oxygen isotopic compositions of multiple stages of silica (chalcedony, quartz, and opal) deposition and

some provisional $^{87}\text{Sr}/^{86}\text{Sr}$ ratios of calcite, and evaluates the apparent timing of latest calcite formation in several occurrences from the ESF based on provisional ^{14}C age determinations. The purpose of this investigation is to use this isotopic characterization of secondary minerals to trace isotopic variations in the water that percolated through the sequence of volcanic rocks at Yucca Mountain and to reconstruct the hydrologic response of Yucca Mountain to past climatic variations. This study focuses mainly on samples obtained in excavations of the ESF and expands interpretations based on earlier studies. Sampling and examination of secondary mineralization within the ESF has increased our understanding of the distribution of secondary minerals and demonstrated a greater extent and thickness of secondary mineral occurrences, the very delicate nature of some of the calcite crystal forms, and a more widespread distribution of opal than had been observed from studies of drill-core occurrences.

Yucca Mountain is located near the western boundary of the Nevada Test Site in southwestern Nevada about 140 km northwest of Las Vegas and lies in the north-central part of the Basin and Range physiographic province. It consists of a series of rugged north-trending fault-block ridges composed of volcanic rocks with a general eastward tilt of 5° to 10° (Scott and Bonk, 1984). A thick section of Tertiary volcanic rocks (table 1) overlies Paleozoic sedimentary strata in the Yucca Mountain region (Byers and others, 1976) with units of the 12.8 to 12.7 Ma Paintbrush Group (Sawyer and others, 1994) forming most exposures (Christiansen and Lipman, 1965; Scott and Bonk, 1984). Two voluminous densely welded ash-flow tuffs of the Paintbrush Group underlie Yucca Mountain (the Tiva Canyon and Topopah Spring Tuffs), separated by a much thinner interval of mostly nonwelded pyroclastic rocks (Buesch and others, 1996); the tuffaceous rocks are greater than 3,000 m thick in some places (Snyder and Carr, 1984). Welding and consolidation of the thick tuffaceous units produced zones of abundant lithophysal cavities, where lithification around gas bubbles formed open cavities in the rock. High-angle faults locally exhibit displacements of several hundred meters (Carr, 1984; Scott and Bonk, 1984); numerous studies (summarized in Volume 1, Part A, of the Site Characterization Plan for Yucca Mountain; U.S. Department of Energy, 1988, section 1.3) have shown that the tectonic setting of Yucca Mountain is complex, with the area situated at the intersection of contrasting structural zones.

This document was originally a milestone report to the Department of Energy Yucca Mountain Project, submitted in June of 1996. This version has benefited from several thorough editorial reviews, but the content herein is consistent with the original 1996 report.

SAMPLE DISTRIBUTION

Since tunneling began in 1995, 145 occurrences of secondary mineralization within the ESF have been collected for the USGS, 88 by the Bureau of Reclamation during fiscal year (FY) 1995 as part of the

Table 1. Major stratigraphic units in the Late Cenozoic volcanic rock sequence of the Yucca Mountain area. Ages are given in millions of years (Ma). Modified from Sawyer and others 91994) and Buesch and others (1996).

Unit	Age (Ma) ¹
Timber Mountain Group	
Ammonia Tanks Tuff	11.45
Rainier Mesa Tuff	11.6
Post-Tiva Canyon pre-Rainier Mesa rhyolites ²	12.5
Paintbrush Group	
Tiva Canyon Tuff	12.7
Yucca Mountain Tuff	--
Pah Canyon Tuff	--
Topopah Spring Tuff	12.8
Calico Hills Formation	12.9
Crater Flat Group	
Prow Pass Tuff	--
Bullfrog Tuff	13.25
Tram Tuff	--
Lithic Ridge Tuff	14.0

¹Ages have not been determined for all units.

²This informal grouping represents multiple rhyolites of small areal extent erupted from multiple sources at the margins of calderas such as the Timber Mountain caldera complex north of Yucca Mountain. Correlations are incompletely understood for all such identified rhyolites and calderas.

Consolidated Sampling Program and 57 during FY 1996 by the USGS (Yucca Mountain Project) Isotope Hydrology Team. The location of the ESF and the locations of newly sampled boreholes (USW SD-7, USW SD-12, USW VH-1, USW VH-2, USW UZ-14, and UE-25 a #5) are shown on figure 1; the

approximate locations of those ESF occurrences that have been sampled are shown on figure 2.

Sampling and analytical methods

Secondary mineral occurrences were examined from drill cores UE-25 a #7, USW UZ-14, USW SD-7, USW SD-12, and USW VH-2 and from underground exposures in the ESF. These samples are tabulated in appendix 2 along with each sample's Hydrogenic Deposits (HD) sample tracking number. Individual occurrences from drill core are designated by borehole name and depth below surface. Position within the ESF is defined by station number (a station is located every 100 m beginning at the North Portal) and incremental distance from the previous station. For instance, an occurrence collected 1456.7 meters from the North Portal would be designated as station 14+56.7. Occurrences within the ESF are listed in appendix 2 by their distance from the North Portal.

Sample textures, morphology, and mineralogy were described from hand specimens and petrographic thin sections. Hand specimens were examined under a stereomicroscope at magnifications up to 75x at visible and short-wave ultraviolet (UV) wavelengths. Minerals were identified by their habit, reaction to hydrochloric acid, hardness, and UV fluorescence. Thick (100- to 200-micrometers) polished sections were prepared from most samples for examination in plane-polarized light and observation of cathodoluminescence (CL) behavior. Scanning-electron microscopic (SEM) observations were made on gold-coated sections and specimen fragments on a Cambridge StereoScan 250 MkII instrument at an accelerating voltage of 20 kV and a working distance of 20 millimeters.

Calcite was sampled from hand specimens for stable isotope analysis by milling with dental burs. Sampling of individual mineralization stages, when such were distinct, was accomplished by milling under low-power magnification. Layers as thin as 0.1 millimeter could be milled from calcite crystal faces and from channels as narrow as 0.5 millimeter within mineral sequences.

Silica minerals were sampled by chipping or gouging from hand specimens or by milling with a diamond-impregnated dental bit. Impurities were removed by hand-picking, and the separates were then digested at room temperature in 0.1 N HCl to remove possible carbonate impurities.

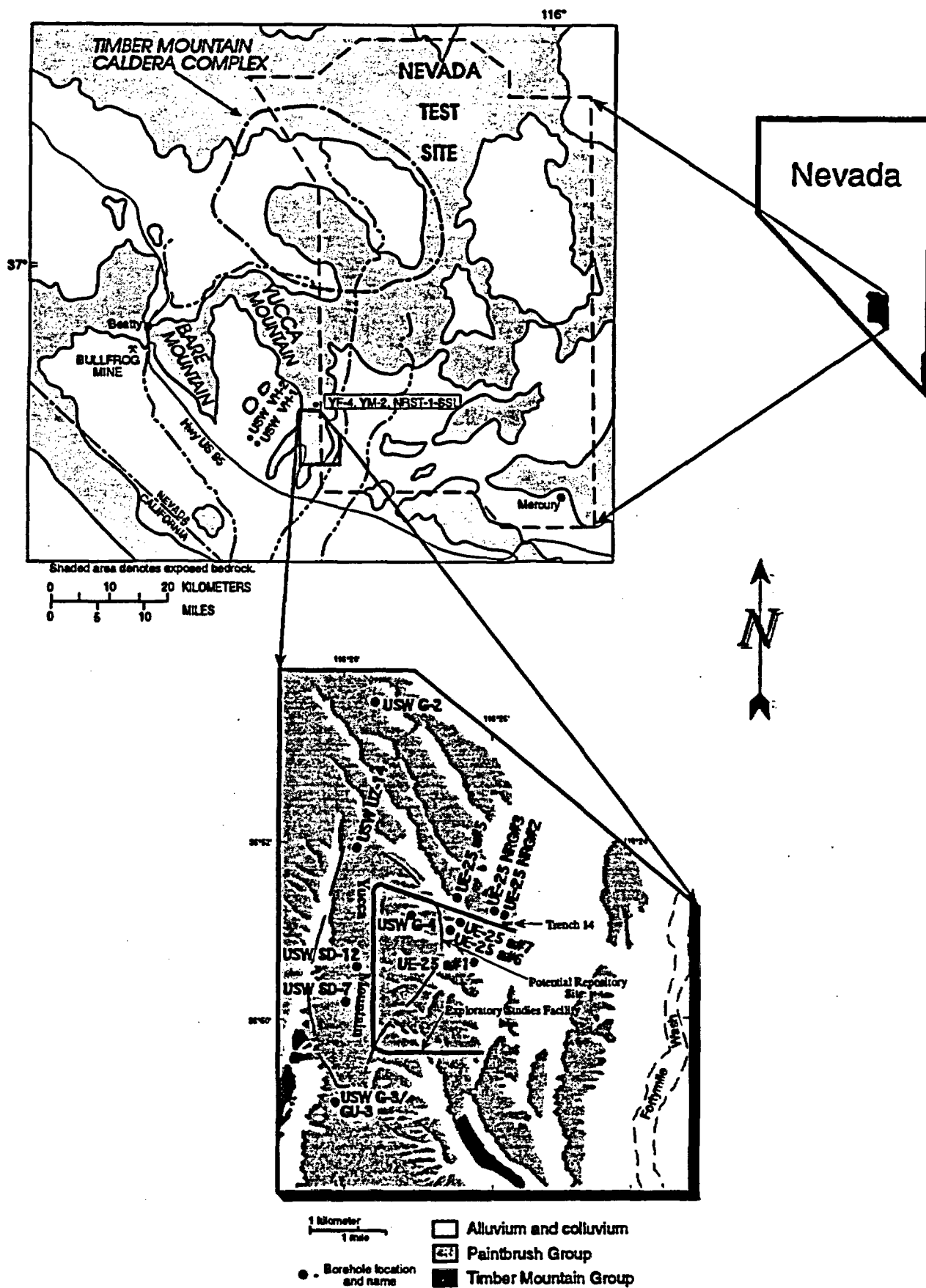


Figure 1. Location of the Yucca Mountain region, Nevada, the potential repository site, the Bullfrog Mine, sampled boreholes, Trench 14, and the Exploratory Studies Facility.

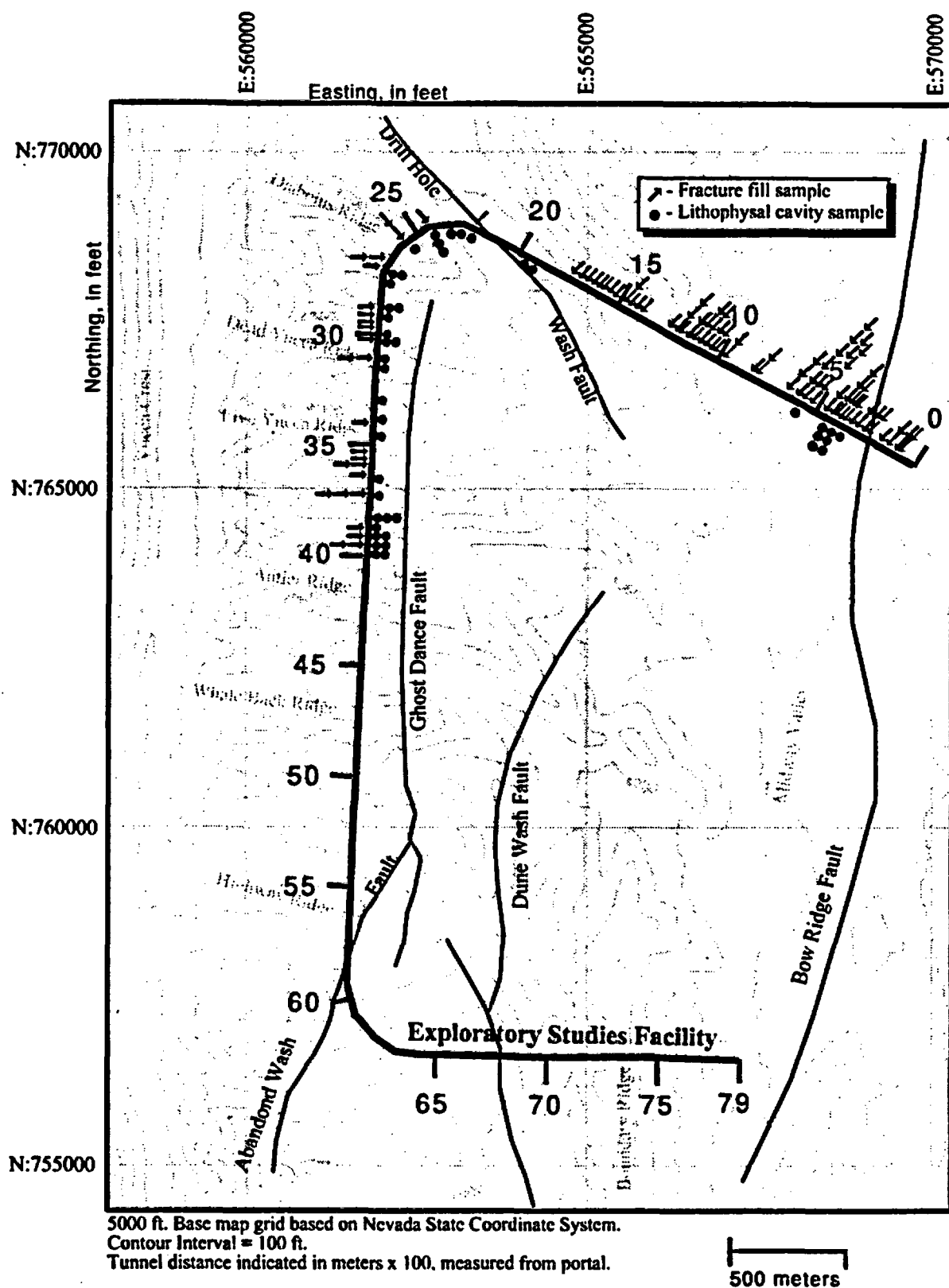


Figure 2. Location of the Exploratory Studies Facility, topographic features, prominent faults, and the locations of sampled secondary mineralization occurrences, near Yucca Mountain, Nevada.

Procedures based on conventional techniques first described by McCrea (1950) were used to extract CO₂ from carbonates. Oxygen was extracted from the silica separates by stepwise fluorination for more highly hydrated opaline separates according to procedures described by Haimson and Knauth (1983), or by reaction with BrF₅ for less-hydrated separates according to procedures developed by Clayton and Mayeda (1963), and converted to CO₂ by reaction with hot graphite. Stable carbon and oxygen isotopic compositions of the extracted CO₂ were determined on Finnigan MAT 251 or 252 mass spectrometers. Stable isotope compositions are reported as the per mil deviations of the samples from the international standards PDB (for carbon) and SMOW (for oxygen). Delta (δ) deviations are defined as

$$\delta = ((R_{\text{sample}} - R_{\text{standard}})/R_{\text{standard}}) \times 1000 \quad (1)$$

where R is the ratio of the heavier isotope (¹³C or ¹⁸O) to the lighter isotope (¹²C or ¹⁶O, respectively) in the sample or standard CO₂. One-sigma reproducibility of the δ¹³C and δ¹⁸O values is routinely less than or equal to 0.1 and 0.15 per mil, respectively.

Ninety-eight aliquots of laboratory standard NBS-19 (or its in-house equivalent, TS-1) analyzed during the course of data collection had average δ¹³C and δ¹⁸O values of 1.91 ± 0.02 per mil and 28.32 ± 0.15 per mil, respectively, compared to accepted values of 1.92 and 28.65 per mil. All δ¹⁸O values reported in appendix 2 have been adjusted by +0.30 per mil to correct the measured deviation from the accepted value for NBS-19.

Strontium isotopic compositions (⁸⁷Sr/⁸⁶Sr) were measured on samples of calcite from the ESF. Small (about 10-mg) subsamples of calcite were milled or chipped from natural or sawn surfaces. The subsamples were leached with hydrochloric acid to remove calcite from opal and wall rock, and any residues were dried and weighed to determine the actual amounts of calcite that was dissolved. Strontium was separated using standard ion-exchange methods, and isotopic compositions were determined on an automated multi-collector solid-source mass spectrometer. The reported ⁸⁷Sr/⁸⁶Sr ratios are within about ± 0.005 per cent of the actual value.

PARAGENESIS OF EXPLORATORY STUDIES FACILITY OCCURRENCES

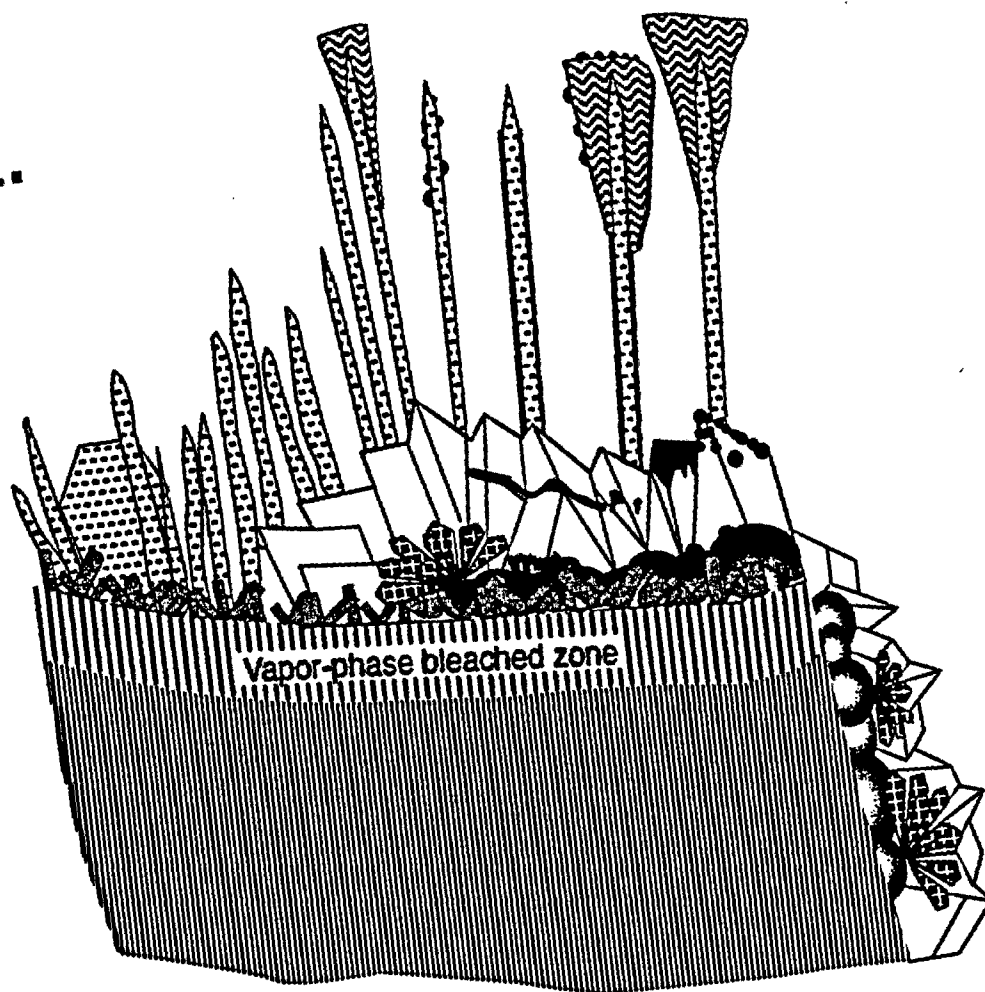
Paragenesis is defined as the order of mineral formation or a characteristic association or occurrence of minerals (Gary and others, 1974). A paragenesis may include a wide variety of minerals or only one or two; it may be simple, or it may be complex with numerous resolvable depositional events. Within a mineralization sequence, many textural relationships may be clear, some may seem clear but are not, and some will be ambiguous. Paragenetic descriptions always contain an element of subjectivity imparted by formulating a genetic framework from empirical observations — they are, as such, interpretative. Appendix 1 lists preliminary descriptions of paragenetic sequences of about 70 samples collected in the ESF during FY 1996 by the USGS. That appendix also contains a brief glossary of some of the terminology used in the following discussion. The occurrences described in appendix 1 represent only about half of the occurrences collected to date (February 1996) from the ESF.

Within the brittle and fractured welded tuffs exposed in the ESF, post-vapor-phase secondary minerals are generally restricted to the footwalls of fractures or the floors of lithophysae. This relation indicates that the fluids that precipitated secondary minerals did not fill these open spaces; that is, those tuffs were not within the saturated zone at the time of secondary mineralization. Mineralizing fluids apparently filled only the smallest-aperture fractures and formed, at most, only shallow pools on the floors of lithophysae.

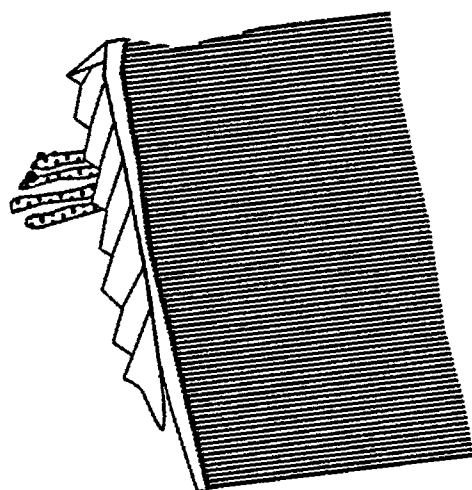
Lithophysal-cavity parageneses differ from those in steeply dipping fractures in that the cavities have thicker accumulations of secondary minerals, they contain larger free-growing crystals of calcite that commonly display unusual bladed habits, and they contain much more opal (figs. 3a and b). Lithophysal-cavity paragenetic sequences begin with vapor-phase tridymite (± hematite), deposited while the tuffs were still hot. Where lithophysae are connected to percolation-flux fracture pathways, those lithophysae may host later calcite and silica minerals.

The earliest secondary mineralization found in such lithophysae consists of massive silica (undifferentiated quartz and chalcedony, possibly with minor opal) with, locally, minor calcite that appears to underlie the massive silica. Calcite, with irregularly

a.



b.









-  early vapor-phase minerals
-  quartz of massive silica stage
-  chalcedony/opal of massive silica stage
-  late bubbly or laminated opal
-  blocky calcite stage
-  bladed calcite and sceptor overgrowths

Figure 3. Schematic illustrations of the typical paragenetic sequences found (a) in lithophysal cavities and (b) on fracture surfaces. Descriptive terminology is defined in the glossary included in Appendix 1.

distributed opal (both in time and space), generally completes the paragenesis. Defined paragenetic stages are, therefore, early massive silica (\pm calcite) and later main-stage calcite (\pm opal). Main-stage calcite and opal, as defined here, are pertinent to model estimations of past flux.

Secondary mineral habits vary somewhat within the main stage of lithophysae. Early main-stage calcite within the lithophysae is commonly blocky or tabular. Later main-stage calcite, however, commonly occurs as unusual bladed crystals, typically thin at the base and flaring outward at the top, a habit that results in a scepter-like cross section (figure 4d). Opal may be found throughout the main stage although it is typically more common in the later part. Opal most commonly occurs as scattered spheres or botryoidal to colloform masses (figures 4a–c) but locally forms thin laminated coatings. Thin-section observations indicate that opal deposition is commonly preceded or accompanied by dissolution of calcite substrates.

Secondary mineral parageneses in steeply dipping fractures differ in habit and mineral abundance from those in lithophysae. Steeply dipping fractures generally contain only blocky to tabular calcite, locally on patches of early-stage massive silica. The sceptered calcite blades and small-bubbled or laminated opal found in lithophysal cavities are rare in steeply-dipping fractures. In the more horizontal fractures, however, the paragenetic sequences are similar to those found flooring lithophysae. This structural control indicates that spatial geometries that retard or halt flow, such as lithophysae or flat-lying fractures, promote formation of the coarse-bladed calcite as well as opal, perhaps because such settings allow solutions to pond and solutes to concentrate through evaporation.

Most Recent Event: Calcite or opal? – Precipitation or dissolution?

Dating the most recent record of percolation fluxes is important for correlation with regional climatic reconstructions and to provide bounds for assessment of performance of a potential repository. Observing the outer, free-growth surface of mineralization and identifying whether calcite or opal was the last-formed mineral seems straightforward, bearing in mind that the most recent evidence of percolation flux might be mineral dissolution. Scanning-electron microscope observations, however, have revealed

complex cycles of latest calcite/opal formation (figures 4a–c). These observations show that most calcite crystal faces appear fresh (figures 4b, d, and g). Some calcite crystal faces, however, appear pitted (figure 4h) which may indicate calcite dissolution (Vaniman and Chipera, 1996). Dating of materials from these outermost surfaces may, therefore, determine the age of most recent mineral deposition or, if the last event was mineral dissolution, the maximum age of the corrosion event. Either age constraint provides useful information, because correlating climatic states with percolation fluxes (and chemistries) that resulted in secondary mineral dissolution is as important as identifying those climates that produced mineralizing percolation.

Dissolution events within the unsaturated zone?

Many secondary mineral occurrences within the ESF, particularly those flooring lithophysae, appear to have been corroded around their basal attachment to the tuffaceous substrate (noted in appendix 1 as "basal dissolution"). This basal dissolution is local, commonly affecting only part of an occurrence that otherwise consists of firmly attached and tightly intergrown calcite crystals with pristine youngest crystal faces. Basal dissolution created voids several millimeters high by centimeters wide, a sort of small-scale cavernous porosity. Some of the calcite remnants in these "dissolution" zones are adorned with tiny, tooth-like, calcite forms that appear to be overgrowths post-dating dissolution (figures 4e and f). In fracture settings, basal dissolution is expressed as loosening of the attaching layer resulting in coatings that lie loosely on the fracture walls.

In many instances, the secondary mineral substrates are more permeable than the secondary mineralization coatings or growths they host, especially the bleached and altered margins associated with vapor-phase mineralization of lithophysae and fractured tuffs. In the laboratory, water dripped onto the bleached margin of a lithophysal cavity moved through the altered matrix and, within seconds, produced obvious wetting of the matrix 10 to 15 centimeters away. The high permeability of the altered rims of lithophysae provides a means for percolating water, perhaps at low flux rates, to contact and dissolve calcite from the base of a lithophysal occurrence without corroding the later calcite in the occurrence.

4a.

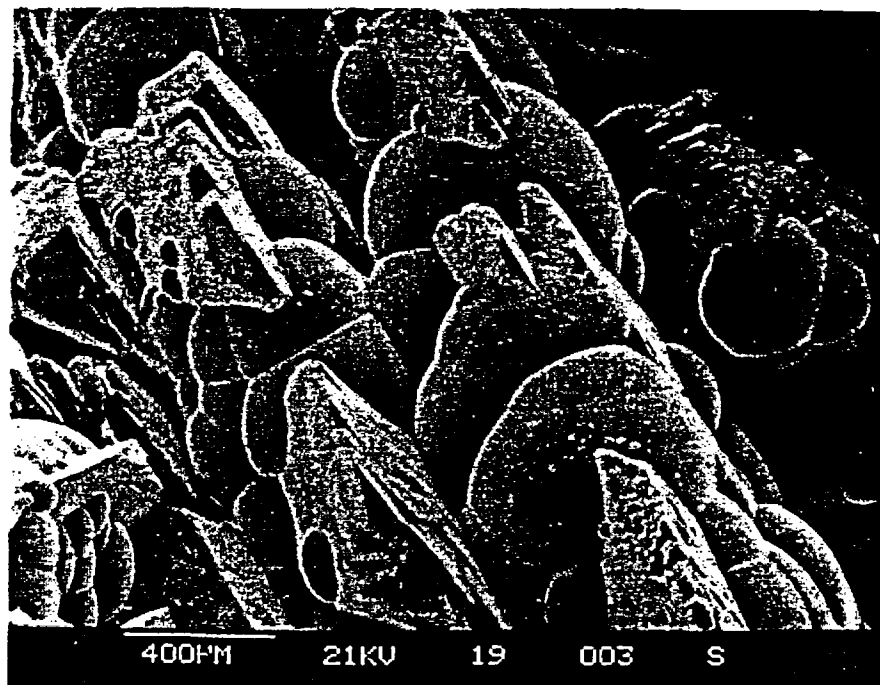


Figure 4a. Photomicrograph of late botryoidal opal with rhombic overgrowths of calcite that are, in turn, locally pimpled with tiny opaline spheres. Scale bar indicates 400 microns.

4b.

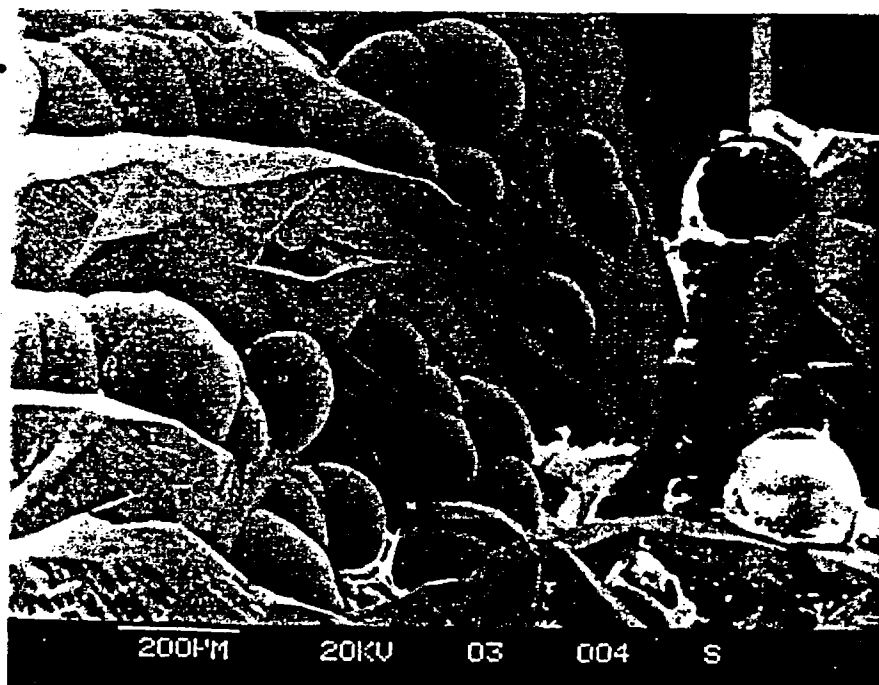


Figure 4b. Photomicrograph of late botryoidal opal on calcite (not shown) partially engulfed by a later stage of calcite. Note the clean uncorroded surfaces of the calcite and opal. Scale bar indicates 200 microns.

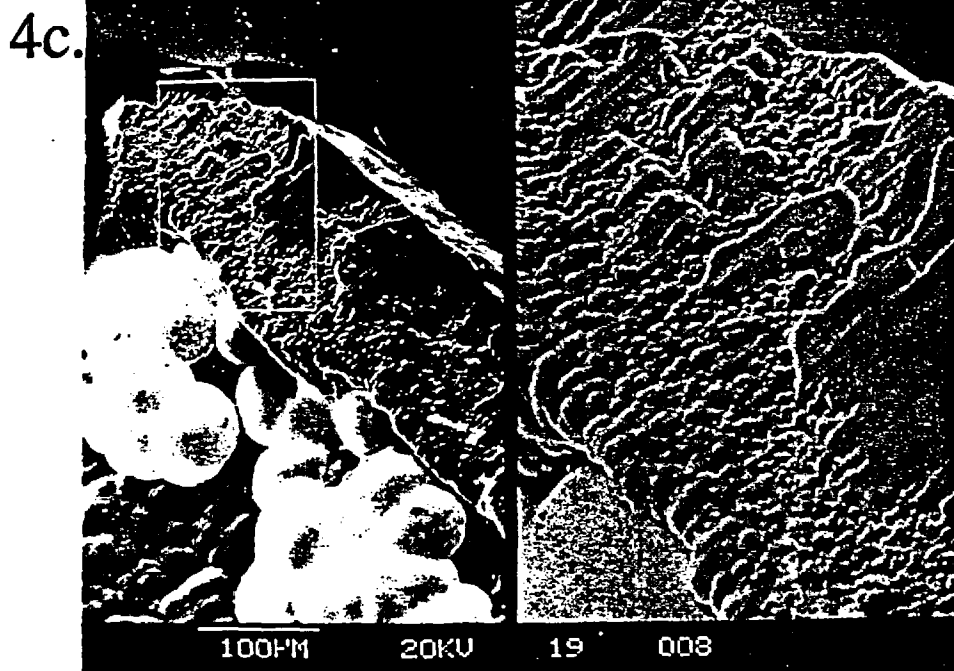


Figure 4c. Photomicrograph of opal (lower left in left image) with overgrowths of a later opaline stage (white spheroids) followed by calcite overgrowth coated with botryoidal opal that is, in turn, partially buried by late calcite. Image on the right is an approximately 3X enlargement of the later mineralization stages. Scale bar indicates 100 microns.

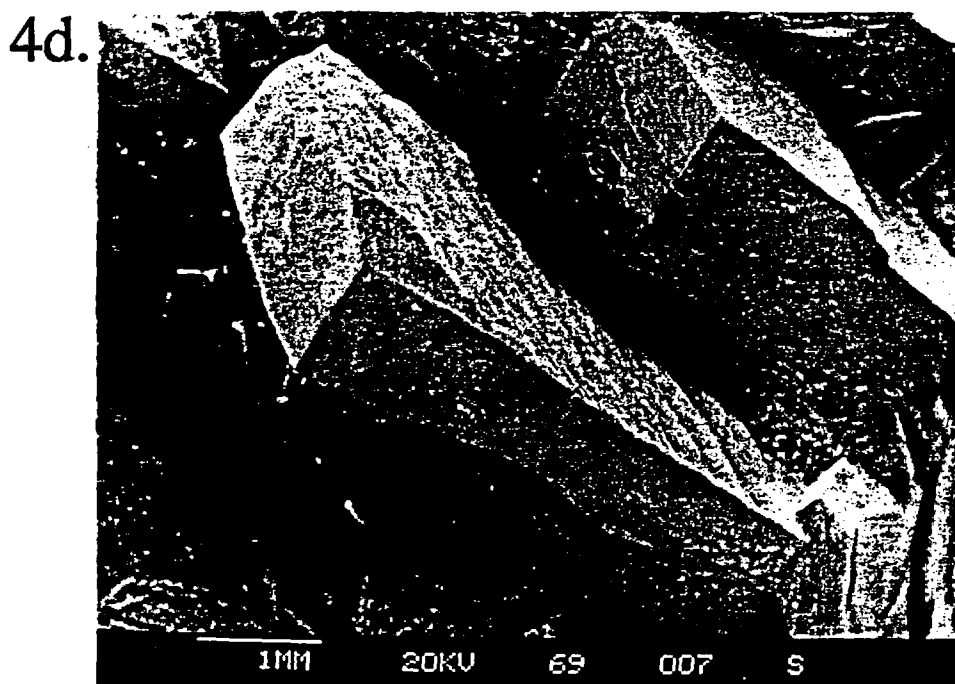


Figure 4d. Photomicrograph of bladed calcite crystals with scepter-like terminations. Scale bar indicates 1 millimeter.

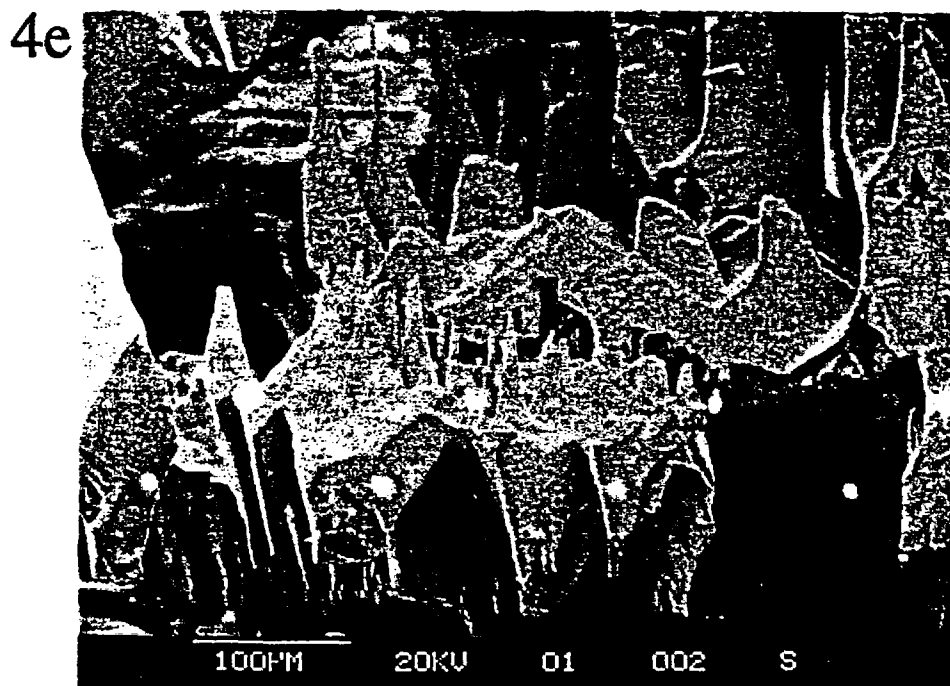


Figure 4e. Photomicrograph of pyramidal to spire-like calcite forms on the basal zone of lithophysal secondary calcite mineralization apparently corroded by later solutions; the relatively fresh faces of this calcite indicate that it may be neofomed and postdate the dissolution event. Scale bar indicates 100 microns.

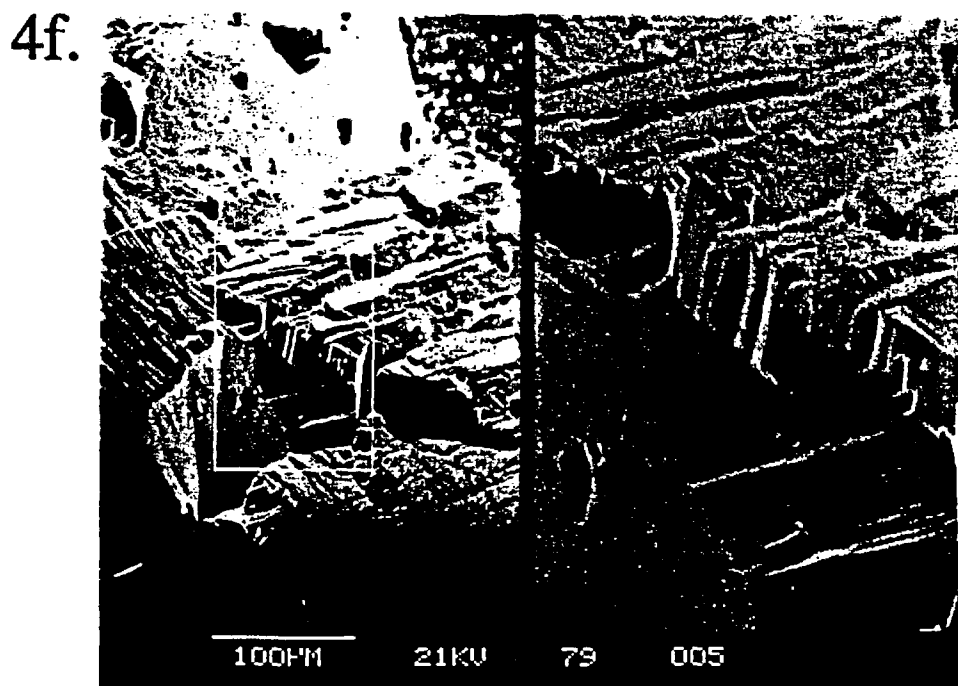


Figure 4f. Photomicrograph of a basal dissolution zone, with delicate forms representing miniature speleothems or meniscus cements. Image on right is an approximately 3X enlargement. Scale bar indicates 100 microns.

4g.

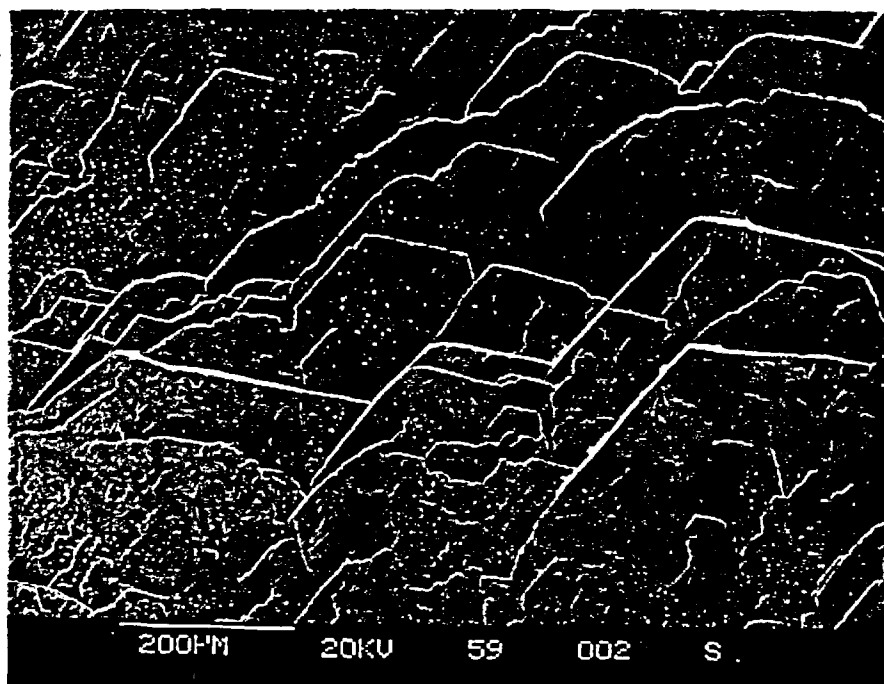


Figure 4g. Photomicrograph of an apparently unetched calcite crystal face. Calcite crystals present a variety of forms but typically appear fresh and unetched in these occurrences. Scale bar indicates 200 microns.

4h.

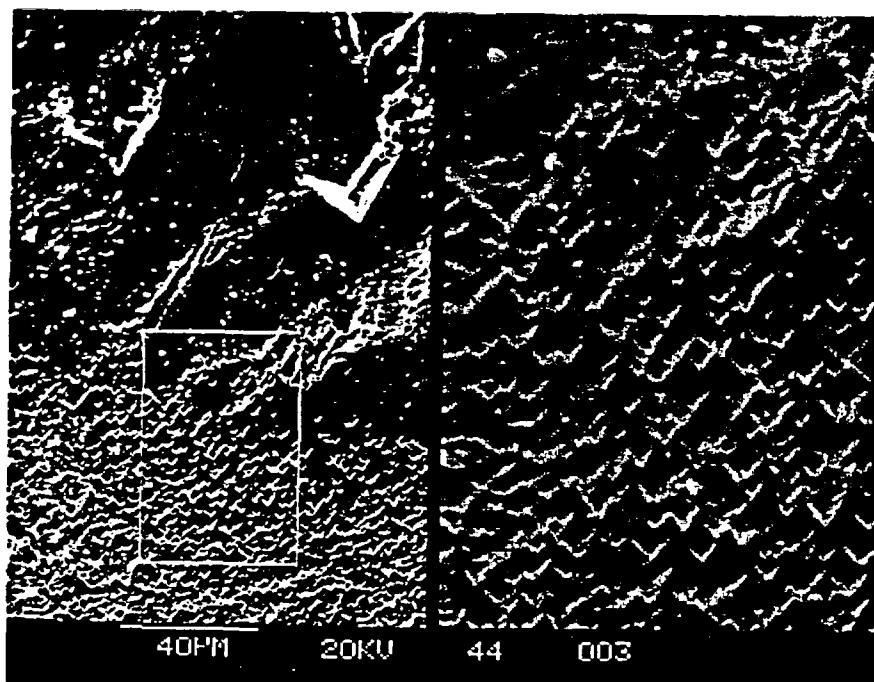


Figure 4h. Photomicrograph of pitted surface of apparently etched calcite crystal face. Image on right is any approximately 3X enlargement of the etched surface. Scale bar indicates 40 microns.

The generalizations discussed here and the specifics listed in appendix 1 are preliminary. Further petrographic and scanning-electron microscopic examination of samples collected during completion of the ESF might provide additional textural constraints that would clarify the hydrologic and geochemical histories of calcite and opal deposition.

ISOTOPIC DATA

Determinations of the $\delta^{13}\text{C}$ and $\delta^{18}\text{O}$ of 310 secondary calcite samples from ESF occurrences and 123 determinations from drill-core occurrences were performed to obtain isotopic characterizations of the secondary calcite (appendix 2). These measurements supplement data from previously published reports (Whelan and Stuckless, 1992; Whelan and others, 1994; Whelan and Moscati, U.S. Geological Survey, written commun., 1997) and are merged with those data on figures 5 and 6. Isotopic data obtained from samples taken from ESF occurrences located between the northern portal and station 40 are listed in appendix 2. Calcite from those ESF occurrences has $\delta^{13}\text{C}$ values ranging from -9 to +8.4 per mil and $\delta^{18}\text{O}$ values ranging from 10.5 to 20.6 per mil (fig. 6). Preliminary determinations of the $^{87}\text{Sr}/^{86}\text{Sr}$ ratio of ESF calcite from occurrences near stations 5, 14, 16, 17, 19, and 30 ranged from 0.70958 to 0.71250.

Implications of new Exploratory Studies Facility data to previous interpretations

Carbon isotopic compositions of unsaturated-zone calcite reflect exchange between infiltrating fluids and components of the overlying soils and are fundamentally controlled by variations in the proportions of C3 and C4 plants that comprise the surface plant community and which vary as a function of climate. Plants photosynthesize via two pathways, designated C3 and C4, which result in markedly different carbon isotopic compositions of about -26 and -13 per mil, respectively (see, for example, Quade and others, 1989). The C4 plants (such as many grasses) favor drier and hotter climates and are better suited to handle those climatic stresses, whereas wetter and milder climates promote growth of woody, herbaceous C3 plants. The isotopic compositions of soil organic matter and respired CO_2 in the soil are, therefore, closely related to climate, and the $\delta^{13}\text{C}$

values of dissolved carbonate in unsaturated-zone percolation (and the calcite formed from it) are a reflection of the climate at the time of infiltration. Oxygen isotopic compositions of unsaturated-zone calcite record the $\delta^{18}\text{O}$ of contemporaneous meteoric waters. The newly obtained $\delta^{13}\text{C}$ and $\delta^{18}\text{O}$ values shown in figures 5 and 6 and tabulated in appendix 2 support the conclusions of Whelan and Stuckless (1992) that unsaturated-zone secondary mineralization formed in a vadose setting, largely from percolation of surface infiltration and at near present-day ambient temperatures. The new data reported here, however, demonstrate a much wider distribution of paragenetically early calcite than previous studies of drill-core occurrences had revealed. The early calcite has higher $\delta^{13}\text{C}$ values that are incompatible with the carbon isotopic compositions of soil-exchanged percolation.

Carbon-13-enriched calcite from the Exploratory Studies Facility

Local occurrences of early calcite from drill-core samples display atypically heavy (^{13}C -enriched) $\delta^{13}\text{C}$ values (fig. 5). Those occurrences (Whelan and Moscati, U.S. Geological Survey, written commun., 1997) also display $\delta^{18}\text{O}$ values that decrease more rapidly with depth, indicating that this early calcite was deposited at warmer temperatures and possibly was subject to a steeper geothermal gradient than prevailed during the formation of later, percolation-deposited calcite.

Exploratory Studies Facility calcite occurrences (fig. 6) more commonly display $\delta^{13}\text{C}$ values greater than 0 per mil than had been observed in drill-core occurrences (fig. 5). Most of that ^{13}C -enriched calcite occurs within the upper half of the Topopah Spring Tuff. Because it is possible to examine and select the most paragenetically complete assemblages when sampling in the ESF, in contrast to the random set of occurrence intersections from drill core, the increased representation of ^{13}C -enriched calcite in the ESF data set could reflect a sampling bias. However, it could as well indicate a real difference between the early hydrologic history of the Topopah Spring Tuff and the other unsaturated zone tuffs. The ^{13}C -enriched calcite is much more common in the non-lithophysal zones than in the upper lithophysal zone of the Topopah Spring Tuff (fig. 6), although the cause of this apparent lithologic control is not clear.

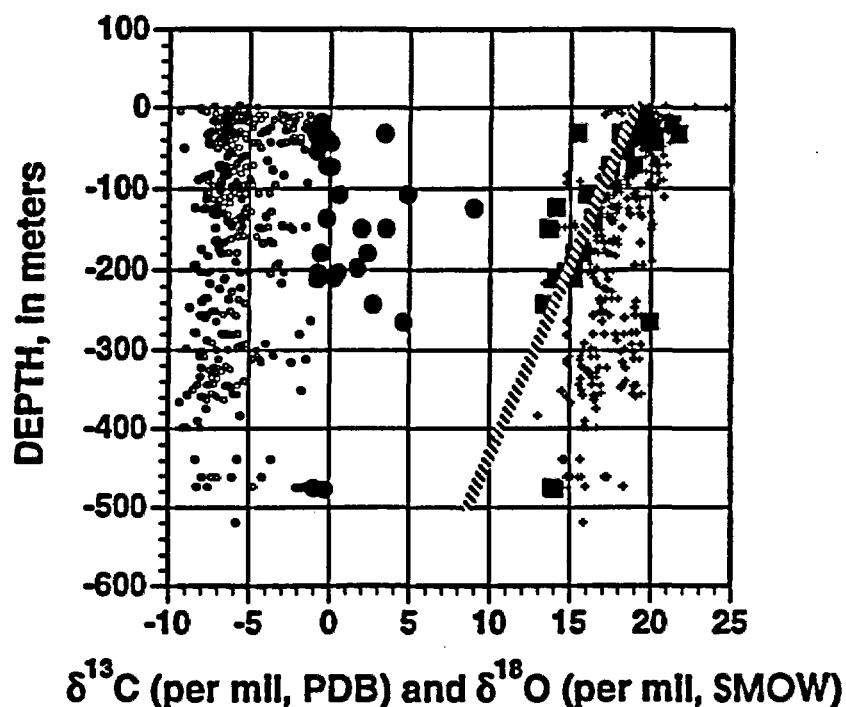


Figure 5. Distribution of unsaturated-zone $\delta^{13}\text{C}$ (o symbol) and $\delta^{18}\text{O}$ (+ symbol) values of calcite plotted against depth (in meters). Occurrences of ^{13}C -enriched paragenetically early calcite are designated by \bullet ($\delta^{13}\text{C}$) and \blacksquare ($\delta^{18}\text{O}$) symbols. The hatched line shows the predicted $\delta^{18}\text{O}$ of calcite precipitated along a hypothetical geothermal gradient of approximately $100^\circ\text{C}/\text{km}$ from a fluid with a $\delta^{18}\text{O}$ of approximately -12.5 per mil.

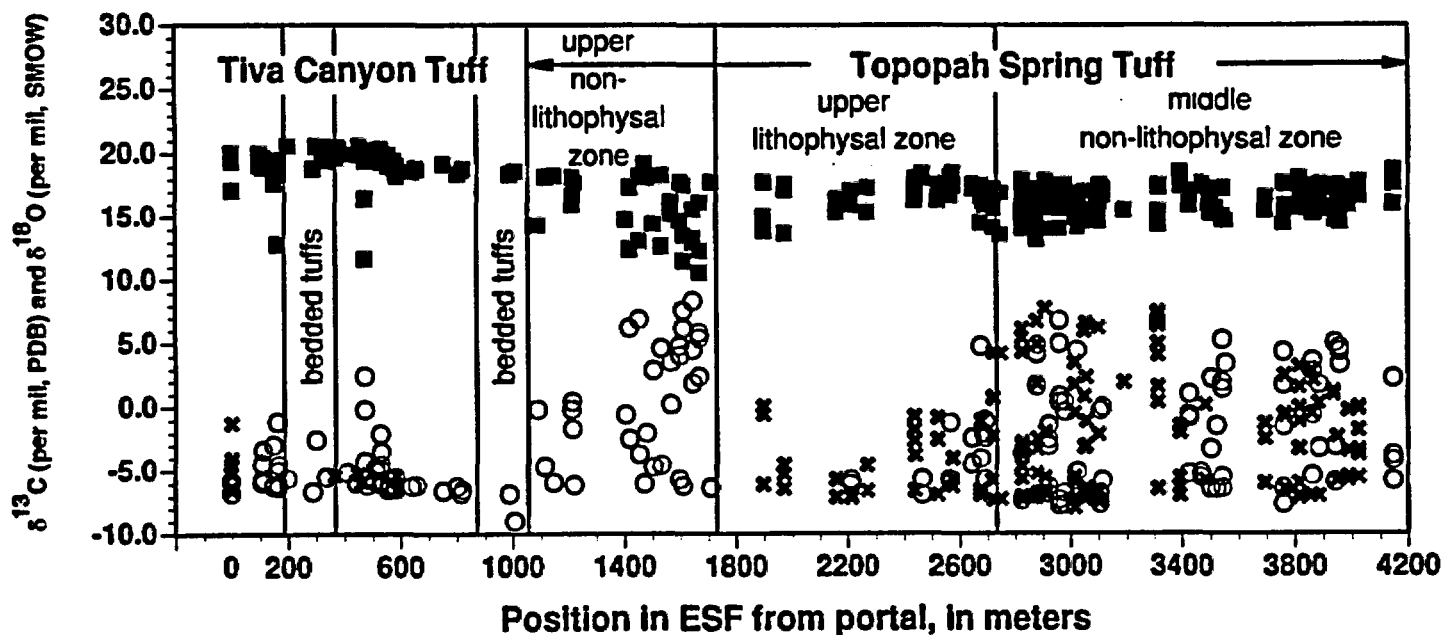


Figure 6. Graph showing $\delta^{13}\text{C}$ and $\delta^{18}\text{O}$ values of Exploratory Studies Facility calcite samples plotted against distance from the portal (station 000). $\delta^{18}\text{O}$ values of all calcite are plotted as \blacksquare . $\delta^{13}\text{C}$ values of a calcite from lithophysal cavities and from fracture coatings are plotted as X and O, respectively.

Provisional measurements of the $^{87}\text{Sr}/^{86}\text{Sr}$ ratios of ESF calcite samples (20 analyses) provide further insight into the origin of the paragenetically early ^{13}C -enriched calcite. Peterman and others (1992) and Marshall and others (1993) concluded that most of the secondary calcite in the unsaturated zone reflects pedogenic strontium sources which have an average $^{87}\text{Sr}/^{86}\text{Sr}$ ratio of 0.71215. Unsaturated-zone calcite occurrences just above the water table, however, had strontium isotopic compositions (average $^{87}\text{Sr}/^{86}\text{Sr}$ value of 0.70909) indicating addition of less-radiogenic strontium, perhaps from the saturated zone. Saturated-zone calcite $^{87}\text{Sr}/^{86}\text{Sr}$ ratios are compatible with derivation of strontium either from the host tuffs of Yucca Mountain or from underlying Paleozoic marine carbonate rocks during an incursion of heated Paleozoic-aquifer water (Marshall and others, 1992), possibly during formation of the Timber Mountain caldera (Broxton and others, 1987; Bish and Aronson, 1993).

Paragenetically early calcite has less-radiogenic $^{87}\text{Sr}/^{86}\text{Sr}$, higher $\delta^{13}\text{C}$, and lower $\delta^{18}\text{O}$, whereas paragenetically later calcite exhibits more-radiogenic $^{87}\text{Sr}/^{86}\text{Sr}$, lower $\delta^{13}\text{C}$, and relatively higher $\delta^{18}\text{O}$ (figs. 7a and b). Whether these trends reflect a continuum of $^{87}\text{Sr}/^{86}\text{Sr}$ ratios, or mixtures of early and late calcite created mechanically during sampling, is not yet clear. It is clear, however, that the less-radiogenic $^{87}\text{Sr}/^{86}\text{Sr}$ ratios may indicate a tuffaceous strontium source for the early calcite as opposed to the more radiogenic pedogenic calcite that appears to provide strontium for the later unsaturated-zone calcite. Furthermore, the rapid decrease of early calcite $\delta^{18}\text{O}$ values with depth indicates a steeper geothermal gradient and warmer fluid temperatures (fig. 5). Both of the above observations are compatible with calcite deposition closely following eruptive activity, when geothermal gradients may have been higher and calcareous soils had not yet formed. Although these preliminary data indicate a distinctly different geochemical environment for the paragenetically early calcite, the distribution of that calcite is still spatially restricted to the footwalls of fractures and the floors of lithophysae. Therefore, other differences aside, the earliest and oldest calcite present in these samples still indicate formation under unsaturated conditions.

Silica-phase oxygen isotope studies

Silica minerals occur throughout the paragenesis. Tridymite formed as a vapor-phase mineral within lithophysal cavities and along cooling joints during initial cooling and outgassing of the tuffs. Chalcedony (cryptocrystalline quartz) and both drusy and coarse euhedral quartz appeared early and generally preceded calcite deposition, whereas opal occurs sporadically within and upon later calcite as laminated coats, botryoidal masses, or isolated hemispherical grains.

The fractionation of ^{18}O between a silica mineral and the mineralizing fluid is determined by temperature; $\delta^{18}\text{O}$ values can be used, therefore, to infer the formation temperatures of such minerals. Histograms of the $\delta^{18}\text{O}$ values of the various silica phases sampled from Yucca Mountain drill cores and outcroppings (appendix 3) display increasing $\delta^{18}\text{O}$ with decreasing temperature (fig. 8). Tridymite $\delta^{18}\text{O}$ values record deposition at high, nearly syn-volcanic, temperatures and low water-to-rock ratios, with $\delta^{18}\text{O}$ values in the range 9 to 17 per mil. Chalcedony, the earliest post-vapor-phase mineral in many occurrences, has $\delta^{18}\text{O}$ values ranging from 5.8 to 17.3 per mil. Quartz, occurring both as early drusy crusts within and upon the chalcedony and as sprays of clear, inclusion-free prismatic crystals as long as 1 cm, has $\delta^{18}\text{O}$ values ranging from 8.6 to nearly 24 per mil. Higher water temperatures are required by the lowest $\delta^{18}\text{O}$ values of both the chalcedony and quartz, likely greater than 120°C ¹ (Moscati and Whelan, 1996). Such temperatures are consistent with formation either

¹ There are no independent constraints on the temperatures of any unsaturated-zone fluids except fluid inclusion studies of late calcite suggesting formation temperatures less than 100°C (Roedder and others, 1994). A fluid $\delta^{18}\text{O}$ of -12.5 per mil is assumed only to permit qualitative comparison of the $\delta^{18}\text{O}$ values of the different silica phases. At cooler temperatures, this is a reasonable assumption, although the $\delta^{18}\text{O}$ of percolation has likely varied by at least ± 2 per mil around this value. At higher temperatures, water exchanges ^{18}O with the rocks that it passes through which results in increased water $\delta^{18}\text{O}$ values. The amount of the increase will be a function of the temperature and the water-to-rock ratio; assuming a value of -12.5 per mil for the heated water produces minimum calculated mineral-formation temperatures. Clayton and others (1972) and Kita and others (1985) are the respective sources of the quartz (and chalcedony)- H_2O and opal- H_2O fractionation factors used to determine formation temperatures.

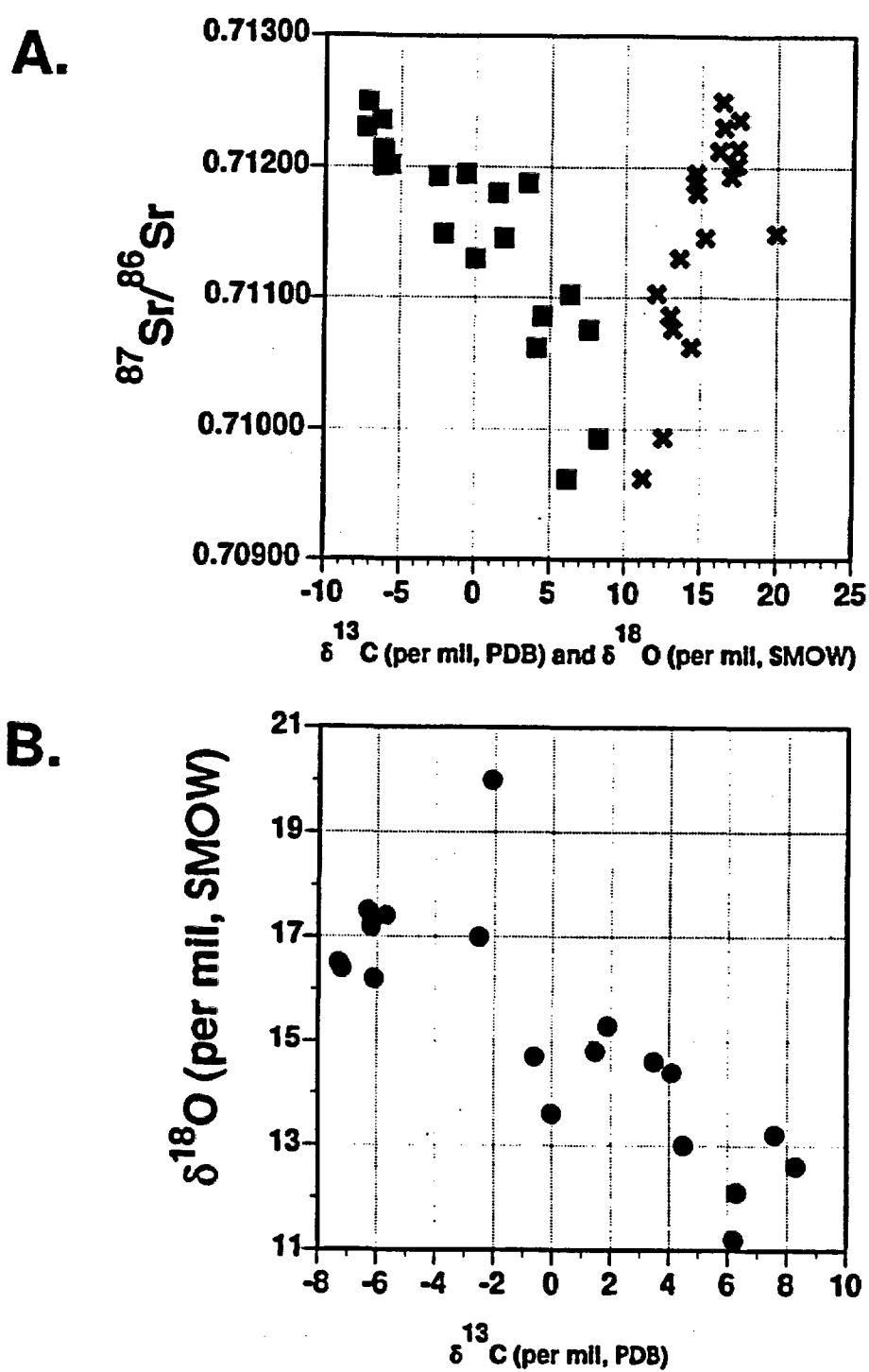


Figure 7. Preliminary radiogenic Sr isotopic compositions plotted against the $\delta^{13}\text{C}$ (■) and $\delta^{18}\text{O}$ (X) isotopic compositions of the Exploratory Studies Facility (ESF) calcite (A), and the correlation between $\delta^{13}\text{C}$ and $\delta^{18}\text{O}$ values of the same ESF calcite (●), shown in (B). In general, larger $\delta^{13}\text{C}$ values correlate with older occurrences.

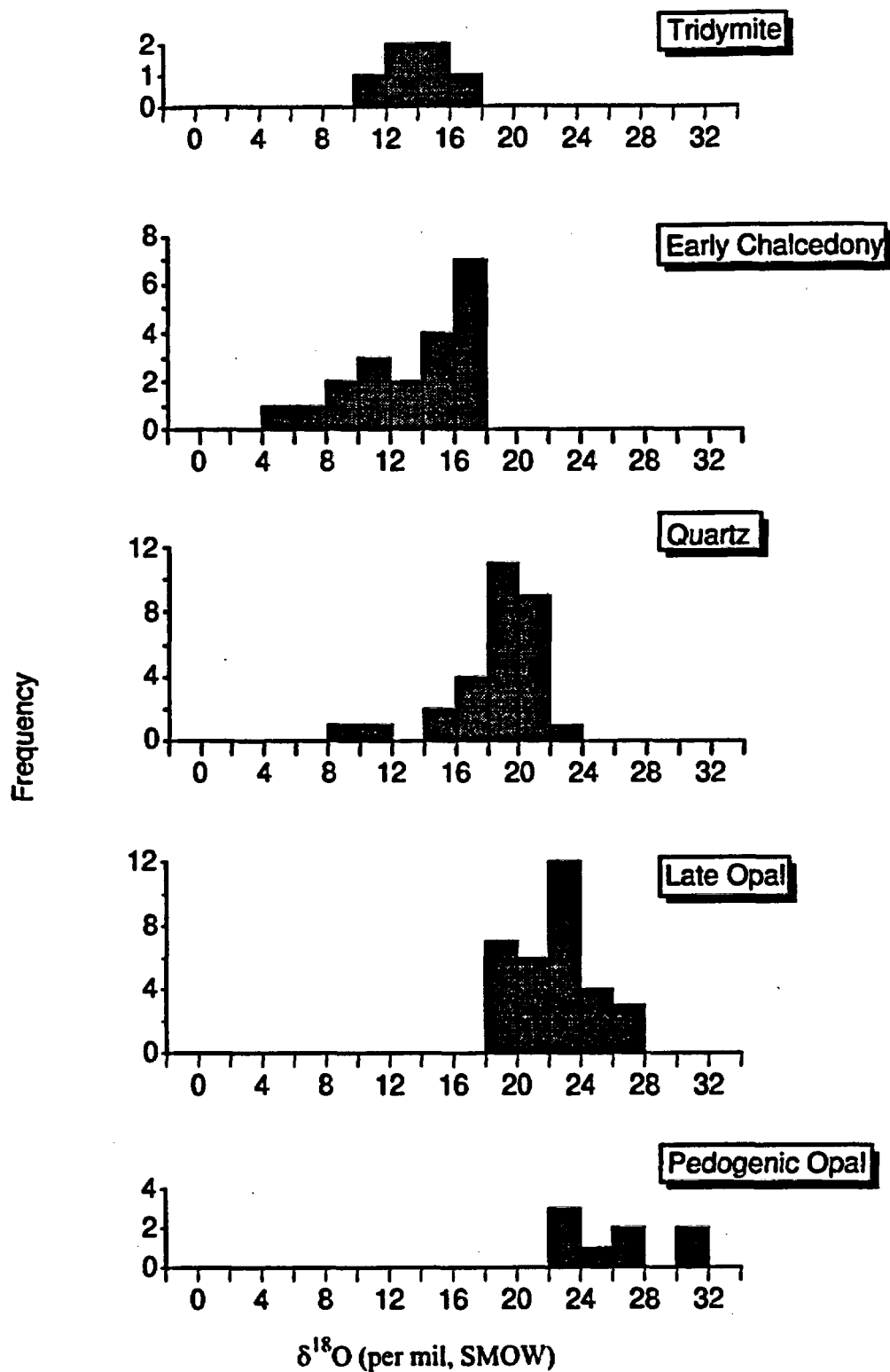


Figure 8. Histograms of Yucca Mountain unsaturated zone secondary silica $\delta^{18}\text{O}$ (per mil, SMOW) values. Relative temperatures of formation and relative ages of silica phases decrease from top to bottom of the figure.

before the host tuff had cooled, or during a later thermal pulse, perhaps accompanying eruption of some of the younger units. Chalcedony and quartz $\delta^{18}\text{O}$ values in the middle part of the observed range require either water temperatures slightly warmer (60 to 70°C) or water $\delta^{18}\text{O}$ values somewhat lower (about 2 per mil) than occur in the unsaturated zone today, whereas the highest quartz $\delta^{18}\text{O}$ values are compatible with present-day water $\delta^{18}\text{O}$ values and temperatures.

Silica mineralization records a wide range of depositional conditions and possibly long depositional history, as well. Whether silica phases also have recorded climatic variability is problematic. Silica phases might have been, occasionally, the dominant secondary minerals forming from percolation, perhaps during times or climates when overlying soils were thin or absent and percolating fluids were deprived of that important source of calcium and carbon for calcite formation.

Opal is the latest silica phase in the unsaturated zone, generally occurring only with calcite. Late opal has $\delta^{18}\text{O}$ values ranging from 18.0 to 27.9 per mil and, assuming water of -12.5 per mil, formed at temperatures of 7 to 45°C (Moscati and Whelan, 1996). Temperatures in the lower part of this range are unlikely. Past variability in $\delta^{18}\text{O}$ values of meteoric water and (or) percolation probably contributed to the relatively large range of opal $\delta^{18}\text{O}$ values.

Pedogenic opal from the overlying soils has the highest $\delta^{18}\text{O}$ values, ranging from 22 to nearly 32 per mil. Assumption of a water $\delta^{18}\text{O}$ value of -12.5 per mil produces estimates that the pedogenic opal formed at temperatures ranging from about 30°C down to an improbable -3°C. Such low estimated temperatures indicate that the opal with the highest $\delta^{18}\text{O}$ values likely was formed from waters with $\delta^{18}\text{O}$ values higher than -12.5 per mil. The ^{18}O -enriched waters might reflect warmer and (or) wetter climates, or evaporative enrichment of the water precipitating pedogenic opal (Moscati and Whelan, 1996).

Silica-mineral $\delta^{18}\text{O}$ values increase from early to late in the paragenetic sequence, implying an overall decrease of depositional temperatures with time. In addition, with the lowest calculated formation temperatures occurring within the overlying soils, opal $\delta^{18}\text{O}$ values conform to increasing temperatures with

depth in the unsaturated zone. Some of the early chalcedony and drusy quartz seem to have formed at somewhat elevated temperatures. Combined with their early position in the paragenesis, this indicates that they formed before the tuffs had completely cooled. Later quartz euhedra, however, appear to have formed at temperatures compatible with the modern geotherm and climate; their water-clear, inclusion-free crystallinity and euhedral habit are consistent with slow growth from relatively cool fluids.

Radiocarbon geochronologic studies

The timing of latest calcite formation in ESF occurrences is being studied with ^{14}C and $^{230}\text{Th}/\text{U}$ geochronometers. Carbon-14 age determinations can be performed on far smaller amounts of calcite than can the $^{230}\text{Th}/\text{U}$ method, an advantage that permits greater sampling resolution. Calcite ^{14}C contents, however, may be susceptible to post-depositional contamination from modern carbon sources such as carbon-bearing fluids or gases in the unsaturated zone. Carbon-14 decays with a half-life of about 5730 years. Although the analytical precision of accelerator mass spectrometry (AMS) is excellent, age determinations begin to lose credibility at ages about 40 ka. At that age, over 99% of the initial ^{14}C has decayed, and minimal contamination by modern ^{14}C can seriously compromise age determinations, especially from small (10- to 30-mg) samples.

Past studies have demonstrated that percolating fluids in the unsaturated zone at Yucca Mountain obtain their $\delta^{13}\text{C}$ signature largely through interaction with carbonate and organic matter in the overlying soils (for example, Whelan and others, 1994). This interaction is characterized by the reaction



in which, as CO_2 is taken into solution, calcite is dissolved. The CO_2 , derived primarily from the oxidation of soil organic matter but secondarily from diffusion of atmospheric gases, is near 100 percent modern carbon (pmc). The calcite dissolved according to equation 2, however, may be old and have 0 pmc ("dead" C), and the HCO_3^- of the resulting solution could have a ^{14}C content as low as 50 pmc; infiltrating

waters could, therefore, have an initial ^{14}C age of one half-life, or about 5700 years. It is unlikely, therefore, that either percolating waters, or calcite precipitated from them in the unsaturated zone, ever record the correct timing of infiltration. Furthermore, the ^{14}C clock for secondary calcite is not set until the calcite is precipitated, so estimates of the timing of infiltration must be adjusted for the travel time of the percolation to the site of deposition.

An ancillary undertaking is to evaluate the likelihood of exchange between the outer surfaces of secondary calcite crystals and later, ^{14}C -bearing, gases and fluids in the unsaturated zone. Such exchange might create a ^{14}C -enriched outer layer on the calcite crystals and, therefore, a young age bias in the ^{14}C data. To test this possibility, the crystal faces of free-growing calcite from several samples were etched briefly with dilute HCl to remove the outer surface. Those etched surfaces were then sampled, as were comparable unetched free-growth calcite surfaces from the occurrence. A minimal difference between these paired ^{14}C age determinations might indicate that post-depositional interaction with rock gases is not a concern. A large difference would be compatible with a thin surface layer of ^{14}C -contaminated calcite on a ^{14}C -“dead” substrate; such a relationship would also, however, be in accord with extremely low calcite depositional rates and most of the ^{14}C -datable calcite record having been removed by the acid etching. This is a moot point, however, in that if calcite depositional rates are that low, then calculated ^{14}C ages are probably unrealistic anyway.

In spite of the stated caveats, ^{14}C dating of calcite still offers useful constraints on the history of percolation flux in the unsaturated zone, primarily because, in many of the occurrences, calcite was the last or only mineral formed. (This is especially true for the fracture occurrences.) Furthermore, because ages can be determined from calcite subsamples as small as 10 mg, ^{14}C permits finer-scale sampling and, therefore, better age resolution of calcite formation than can other dating techniques.

To date, subsamples submitted for ^{14}C AMS age determination have come from (1) the latest surfaces of free-growth calcite crystals or (2) the basal zones of calcite dissolution present in many samples. All of the subsamples from zones of basal dissolution contain a mixture of the “late” overgrowths and the residual, possibly ^{14}C -dead, calcite substrate. These subsamples should still provide an indication, however, of whether a given dissolution event occurred within the past 40 ka, and the subsamples are therefore significant for reconstruction of hydrology/climate interactions in the recent past.

Provisional results of the ^{14}C geochronometry indicate calculated ^{14}C ages (radiocarbon years) in a range from greater than 16 ka to about 42 ka (fig. 9). A significant percentage of the samples showed calculated ages less than 32 ka, indicating a significant component of modern carbon. This relation implies that much of the secondary calcite sampled in the ESF contains at least thin layers deposited during or since the last glacial cycle, and that calcite ^{14}C measurements provide at least a relative tool for spatial and temporal mapping of percolation pathways within the unsaturated zone at Yucca Mountain.

None of the data (shown in appendix 3 and fig. 8) discussed here tested the possibility of surface-layer ^{14}C contamination in ESF samples. Samples of thick mammillary calcite crusts, however, collected from the unsaturated zone of the Sterling Mine on Bare Mountain (fig. 1) west of Yucca Mountain, were tested. Opposite halves of a sawn specimen were ground and polished to reveal the growth banding. One half was briefly etched in dilute (0.2 N) HCl, then both were washed ultrasonically in deionized water, and the youngest band of calcite was milled from each half. The acid-etched sample had an apparent ^{14}C age of 15.3 ± 0.12 ka, whereas the unetched sample gave an age of 14.7 ± 0.12 ka. The minimal difference between the two ages provides little support for post-depositional exchange between modern carbon and unsaturated-zone gases or fluids during the past 15 ky, at least at Bare Mountain.

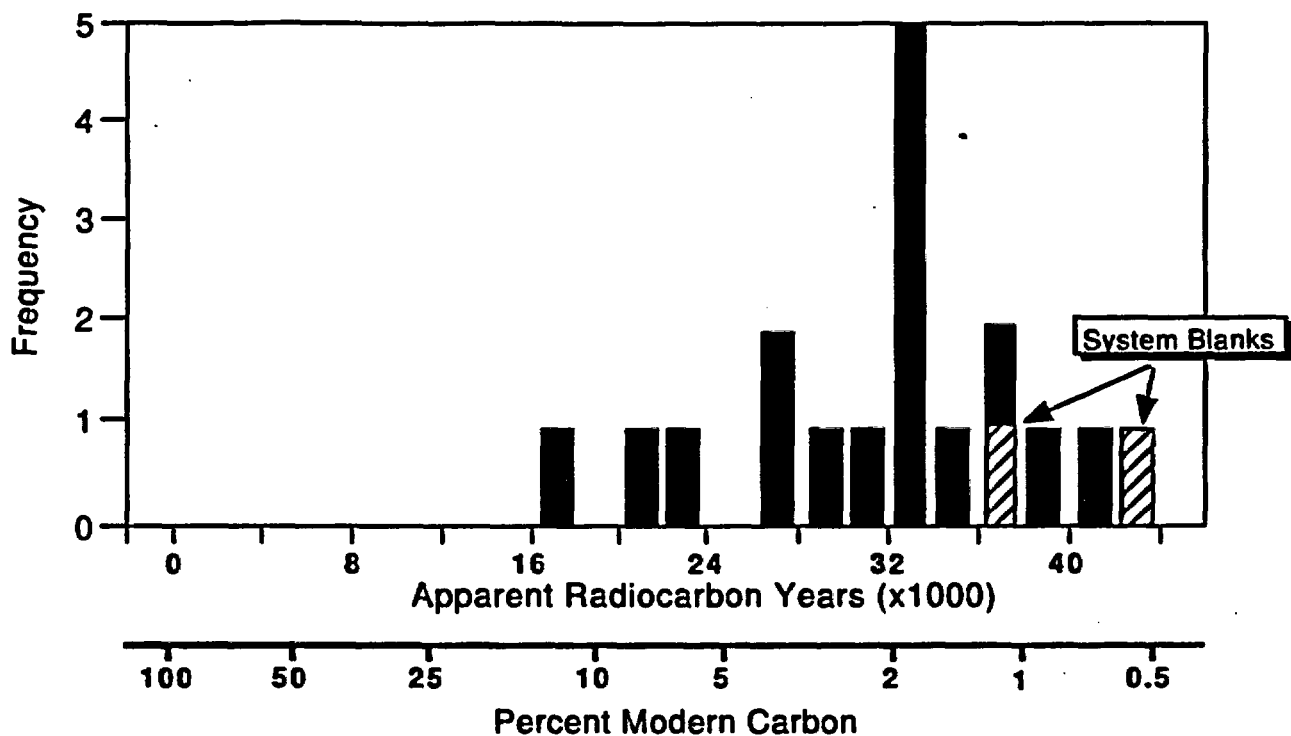


Figure 9. Histogram showing the distribution of ^{14}C ages from the Exploratory Studies Facility calcite occurrences. Upper x-axis shows the apparent age calculated from measured percentages of modern carbon in the sample; no attempt was made to correct for incorporation of dead carbon or ground-water travel time. Lower x-axis displays the relationship between percent modern carbon and apparent age, and underscores the large error that trace amounts of ^{14}C contamination cause in older materials. System blanks are the amounts of ^{14}C measured in samples of Paleozoic calcitic marble subjected to the entire extraction and Accelerator Mass Spectrometer analysis process.

CONCLUSIONS

1. Post-vapor-phase secondary mineralization in the unsaturated zone consisted of an early stage dominated by silica deposition, locally with coeval or possibly precursor calcite, followed by main-stage calcite and opal. Main-stage mineralization, as defined herein, groups all early-stage calcite and opal deposition. This is probably a simplification, and further study might reveal a more complex depositional history.

2. Early calcite is characterized by heavy $\delta^{13}\text{C}$ values and $\delta^{18}\text{O}$ values that increase more rapidly with depth than those of main-stage calcite. Coupled with its association with formation of early chalcedony and quartz, this relation may indicate that the early calcite formed at somewhat higher temperatures than the main-stage calcite and that early calcite should not be included in estimates of past percolation fluxes based on the secondary mineral record.

3. Preliminary strontium isotope analyses indicate that the early calcite contains less radiogenic strontium than does the main-stage calcite. Rather than a pedogenic strontium source as is the case for the main stage, the tuffs themselves may have been the source of strontium in the early calcite.

4. Delta- ^{18}O values of the silica phases quartz, chalcedony, and opal indicate that some of the early massive-silica-stage phases must have formed from heated water, although parts of the massive-silica stage are compatible with modern or near-modern rock temperatures. Opal $\delta^{18}\text{O}$ values argue that evaporative processes increased the $\delta^{18}\text{O}$ of the precipitating water in the soil zone.

5. Preliminary radiocarbon age determinations argue that *in situ* interactions with later carbon-bearing water and gases have not significantly altered the ^{14}C ages of the calcite. Radiocarbon ages of the latest calcite in many of the occurrences may indicate relatively recent formation of the outermost calcite layers.

REFERENCES CITED

- Bish, D.L. and Aronson, J.L., 1993, Paleogeothermal and paleohydrologic conditions in silicic tuff from Yucca Mountain, Nevada: *Clays and Clay Minerals*, v. 41, no. 2, p. 148–161.
- Broxton, D.E., Bish, D.L., and Warren, R.G., 1987, Distribution and chemistry of diagenetic minerals at Yucca Mountain, Nye County, Nevada: *Clays and Clay Minerals*, v. 35, no. 2, p. 89–110.
- Buesch, D.C., Spengler, R.W., Moyer, T.C., and Geslin, J.K., 1996, Revised stratigraphic nomenclature and macroscopic identification of lithostratigraphic units of the Paintbrush Group exposed at Yucca Mountain, Nevada: U.S. Geological Survey Open-File Report 94–469, 47 p.
- Byers, F.M., Jr., Carr, W.J., Orkild, P.P., Quinlivan, W.D., and Sargent, K.A., 1976, Volcanic suites and related cauldrons of Timber Mountain-Oasis Valley caldera complex, southern Nevada: U.S. Geological Survey Professional Paper 919, 70 p.
- Carr, W.J., 1984, Regional structural setting of Yucca Mountain, southwestern Nevada, and Late Cenozoic rates of tectonic activity in parts of the southwestern Great Basin, Nevada and California: U.S. Geological Survey Open-File Report 84–854, 109 p.
- Christiansen, R.L., and Lipman, P.W., 1965, Geologic map of the Topopah Spring NW quadrangle, Nye County, Nevada: U.S. Geological Survey Geological Quadrangle Map GQ–444, scale 1:24,000.
- Clayton, R.N., and Mayeda, T.K., 1963, The use of bromine pentafluoride in the extraction of oxygen from oxides and silicates for isotopic analysis: *Geochimica et Cosmochimica Acta*, v. 27, no. 1, p. 43–52.
- Clayton, R.N., O'Neil, J.R., and Mayeda, T.K., 1972, Oxygen isotope exchange between quartz and water: *Journal of Geophysical Research*, v. 77, p. 3057–3067.
- Gary, M., McAfee, R., Jr., and Wolf, C.L., 1974, Glossary of Geology: American Geological Institute, Washington, D.C., 805 p.
- Haimson, M., and Knauth, L.P., 1983, Stepwise fluorination — A useful approach for the isotopic analysis of hydrous minerals: *Geochimica et Cosmochimica Acta*, v. 47, no. 9, p. 1589–1595.
- Kita, I., Taguchi, S., and Matsubaya, O., 1985, Oxygen isotope fractionation between amorphous silica and water at 34–93°C: *Nature*, v. 314, no. 6006, p. 63–64.
- Marshall, B.D., Peterman, Z.E., and Stuckless, J.S., 1993, Strontium isotopic evidence for a higher water table at Yucca Mountain, *in* High Level Radioactive Waste Management, Proceedings of the Fourth Annual International Conference, Las Vegas, Nevada, April 26–30, 1993: LaGrange Park, Illinois, American Nuclear Society, v. 2, p. 1948–1952.

- Marshall, B.D., Whelan, J.F., Peterman, Z.E., Futa, K.F., Mahan, S.A., and Stuckless, J.S., 1992, Isotopic studies of fracture coatings at Yucca Mountain, Nevada, in Kharaka, Y.K., and Maest, A.S., eds., *Proceedings of the Seventh International Symposium on Water/Rock Interaction*, Park City, Utah, p. 737–740.
- McCrea, J.M., 1950, The isotopic chemistry of carbonates and a paleotemperature scale: *Journal of Chemical Physics*, v. 18, no. 8, p. 849–857.
- Moscatti, R.J., and Whelan, J.F., 1996, Origin of secondary silica within Yucca Mountain, Nye County, southwestern Nevada: U.S. Geological Survey Open-File Report 95–289, 14 p.
- Peterman, Z.E., Stuckless, J.S., Marshall, B.D., Mahan, S.A., and Futa, K.A., 1992, Strontium isotope geochemistry of calcite fracture fillings in deep core, Yucca Mountain, Nevada—a progress report, in *High Level Radioactive Waste Management, Proceedings of the Third Annual International Conference*, Las Vegas, Nevada, April 12–16, 1992: LaGrange Park, Illinois, American Nuclear Society, v. 2, p. 1582–1586.
- Quade, Jay, Cerling, T.E., and Bowman, J.R., 1989, Systematic variations in the carbon and oxygen isotopic composition of pedogenic carbonate along elevation transects in the southern Great Basin, United States: *Geological Society of America Bulletin*, v. 101, no. 4, p. 464–475.
- Roedder, Edwin, Whelan, J.F., and Vaniman, D.T., 1994, Fluid inclusion homogenization and crushing studies of calcite veins from Yucca Mountain, Nevada, tuffs: Environment of formation, in *High-Level Radioactive Waste Management, Proceedings of the Fifth Annual International Conference*, Las Vegas, Nevada, May 22–26, 1994: LaGrange Park, Illinois, American Nuclear Society, v. 4, p. 1854–1860.
- Sawyer, D.A., Fleck, R.J., Lanphere, M.A., Warren, R.G., Broxton, D.E., and Hudson, M.R., 1994, Episodic caldera volcanism in the Miocene southwestern Nevada volcanic field—revised stratigraphic framework, $^{40}\text{Ar}/^{39}\text{Ar}$ geochronology, and implications for magmatism and extension: *Geological Society of America Bulletin*, v. 106, p. 1304–1318.
- Scott, R.B., and Bonk, Jerry, 1984, Preliminary geologic map of Yucca Mountain, Nye County, Nevada, with geologic sections: U.S. Geological Survey Open-File Report 84–494, scale 1:12,000.
- Snyder, D.B., and Carr, W.J., 1984, Interpretation of gravity data in a complex volcano-tectonic setting, southwestern Nevada: *Journal of Geophysical Research*, v. 89, p. 10193–10206.
- United States Department of Energy, 1988, Site characterization plan, Yucca Mountain site, Nevada Research and Development Area, Nevada: U.S. Department of Energy, Office of Civilian Radioactive Waste Management, document DOE/RW0199, 8 volumes.
- Vaniman, D.T., and Chipera, S.J., 1996, Paleotransport of lanthanides and strontium recorded in calcite compositions from tuffs at Yucca Mountain, Nevada, USA: *Geochimica et Cosmochimica Acta*, v. 60, no. 22, p. 4417–4433.
- Whelan, J.F., and Stuckless, J.S., 1990, Reconnaissance $\delta^{13}\text{C}$ and $\delta^{18}\text{O}$ data from Trench 14, Busted Butte, and drill hole G–4, Yucca Mountain, Nevada Test Site, in *High Level Radioactive Waste Management, Proceedings of the International Topical Meeting*, Las Vegas, Nevada, April 8–12, 1990: LaGrange Park, Illinois, American Nuclear Society, v. 2, p. 930–934.
- Whelan, J.F., and Stuckless, J.S., 1992, Paleohydrologic implications of the stable isotopic composition of secondary calcite within the Tertiary volcanic rocks of Yucca Mountain, Nevada, in *High Level Radioactive Waste Management, Proceedings of the Third Annual International Conference*, Las Vegas, Nevada, April 12–16, 1992: LaGrange Park, Illinois, American Nuclear Society, v. 2, p. 1572–1581.
- Whelan, J.F., Vaniman, D.T., Stuckless, J.S., and Moscatti, R.J., 1994, Paleoclimatic and paleohydrologic records from secondary calcite: Yucca Mountain, Nevada, in *High Level Radioactive Waste Management, Proceedings of the Fifth Annual International Conference*, Las Vegas, Nevada, May 22–26, 1994: LaGrange Park, Illinois, American Nuclear Society, v. 4, p. 2738–2745.

APPENDIX

Appendix 1. Paragenetic sequences of secondary mineral occurrences within the Exploratory Studies Facility (ESF), Yucca Mountain, Nevada

Sample #	ESF Location*	Type	Basal Dissolution	
2021	12+21.83	fracture		msv silica - cal & opal
2022	12+44.25	fracture		msv silica - (bubbly opal)
2023	14+06.0	fracture		blocky to bladed cal - bubbly opal
2001	14+20	fracture	calcite	(anhedral cal) - msv silica - fluorite - bladed cal - bubbly opal
2025	14+55	fracture		msv silica + cal - blocky cal - (opal)
2026	14+72.53	fracture		msv silica - bladed cal
2027	14+79.55	fracture		msv silica - blocky cal - fluorite - bladed cal
2028	15+05.25	fracture		msv silica - blocky cal - fluorite - bladed cal
2029	15+33.25	fracture		anhedral cal - msv silica - blocky cal - fluorite - (opal) - cal o'gth
2030	15+68.58	fracture		(anhedral cal) - msv silica - bladed cal
2002	15+99.95	fracture	calcite	(anhedral cal) - fluorite - msv silica - blocky cal & fluorite - bladed cal
2003	16+12.38	fracture		anhedral cal ± fluorite ± msv silica (paragenesis unclear) - late bladed cal
2004	16+46.6	fracture	(calcite)	(calcite) - msv silica - (blocky cal) - bladed cal
2032	16+70.1	fracture		wall-to-wall cal vein - cal + (opal)
2005	17+10.95	fracture	(calcite)	cal (breccia cement) - (blocky cal) - bladed cal
2006 (1)	19+00.0	litho cavy		vapor phase - blocky cal - bubbly opal - (zeolite) - bladed cal - bubbly opal - cal o'gths - (bubbly opal)
2006 (2)	19+00.0	fracture		blocky cal - bladed cal
2075	19+75	litho cavy	calcite	vapor phase - blocky cal - bladed cal - bubbly opal - blocky cal - bladed cal - bubbly opal
2007-1	22+13.0	fracture		blocky cal - msv silica - bladed cal - bubbly opal - cal o'gths - (late opal)
2007-2	22+13.0	litho cavy		vapor phase - blocky cal - bladed cal - bubbly opal
2008	22+72	litho cavy	calcite	vapor phase - blocky cal - (opal) - blocky cal - bubbly opal - cal o'gths - bubbly opal
2020 (2)	24+37.6	litho cavy	calcite	vapor phase - blocky cal - bubbly opal
2020 (1)	24+39.58	litho cavy	calcite	vapor phase - blocky cal
2020 (3)	24+41.6	litho cavy	calcite	vapor phase - blocky cal - bubbly opal
2009	24+43.50	litho cavy		vapor phase - blocky cal - bubbly opal - (cal o'gths)
2010	24+68.2	fracture		blocky cal - bladed cal
2011	25+68.0	fracture	calcite	blocky cal - bladed cal - scepter o'gths
2012 (1)	25+76.7	fracture	calcite	blocky cal
2012 (2)	25+76.7	int. frac+litho	calcite	vapor phase - blocky cal
2012 (3)	25+76.7	litho cavy	calcite	vapor phase - blocky cal - sparse opal - blocky cal - bladed cal
2013	26+78.58	fracture		blocky cal - bubbly opal - blocky cal
2014	26+88	fracture		blocky cal - bladed cal - opal coat - cal o'gths
2015	26+95.00	fracture	calcite	blocky cal - opal - blocky to bladed cal
2016	27+18.38	litho cavy	calcite	blocky cal - msv silica - blocky cal - bladed cal - bubbly opal - (scepter) o'gths
2017	27+24	litho cavy	(calcite)	vapor phase - blocky cal - bubbly opal - bladed cal - (scepter o'gths) - bubbly opal ± fluorite - cal o'gths

Appendix 1. Paragenetic sequences of secondary mineral occurrences within the Exploratory Studies Facility (ESF), Yucca Mountain, Nevada (Continued)

Sample #	ESF Location*	Type	Basal Dissolution	
2018	27+50.65	litho cavy		blocky cal - opal - bladed cal
2019	28+80	litho cavy		vapor phase - msv silica - bladed cal - botry'l opal - bladed cal - bubbly opal - multi-stage cal (incl'g scepters) + bubbly opal
2019	28+81	litho cavy		vapor phase - msv silica - bladed cal - botry'l opal - bladed cal - bubbly opal - multi-stage cal (incl'g scepters) + bubbly opal
2054	28+81.6	fracture		blocky cal - msv silica - bladed cal - msv silica - bladed cal - opal - zeolite - scepter o'gths
2055	29+11.2	litho cavy		anhedral cal - (bubbly opal) - blocky cal - msv silica - bladed cal - bubbly opal - bladed cal - bubbly opal - cal o'gths
2056	29+22.9	fracture	calcite	anhedral cal - blocky cal - botry'l opal - bladed cal - scepter cal - bubbly opal
2057	29+62.2	fracture	calcite	vapor phase - blocky cal - msv silica - bladed cal - opal coat - scepter o'gth - bubbly opal - cal o'gth - bubbly opal
2058	29+79.98	fracture	calcite	vapor phase - blocky cal - msv silica - bladed cal - bubbly opal - scepter o'gth - (opal coat)
2059	30+17.78	litho cavy	silica, calcite	vapor phase - msv silica - blocky cal - bladed cal - opal coat - scepter o'gth - bubbly opal - cal o'gth - bubbly opal
2060	30+26.58	fracture ?	calcite	vapor phase - (blocky cal) - bladed cal - scepter cal
2074	30+50.7	litho cavy	calcite	vapor phase - blocky cal - msv silica - blocky cal - msv silica - bladed cal - bubbly opal - bladed cal - scepter cal o'gth - bubbly opal - (cal o'gths) - (bubbly opal)
2061	30+57.68	litho cavy	(calcite)	vapor phase - msv silica - blocky cal - bladed cal - msv silica - blocky to bladed cal - bubbly opal - cal o'gths
2073	31+03	litho cavy	calcite	vapor phase - bladed cal - zeolite + opal - bladed cal - scepter cal o'gth - bubbly opal - cal o'gth - bubbly opal
2062	31+07.4	fracture		blocky cal - bladed cal - opal coat - scepter cal o'gth - bubbly opal - cal o'gth - bubbly opal
2063	31+16.1	fracture		blocky cal - bladed cal - scepter o'gths - bubbly opal
2064	31+95.7	litho cavy		vapor phase - blocky cal - (msv silica) - bladed cal - opal coat - cal o'gth
2065	33+16.2	litho cavy	calcite	vapor phase - blocky cal - msv silica ± fluorite - blocky cal - fluorite - bladed cal - opal coat - cal o'gth
2066	33+95.78	litho cavy	calcite	vapor phase - msv silica - blocky cal - bladed cal - opal - cal o'gth - bubbly opal - cal o'gths
2067	34+28.18	fracture		vapor phase - blocky cal - bladed cal
2068	34+86.48	litho cavy	(calcite)	vapor phase - msv silica - blocky cal - bladed cal - bubbly opal - cal o'gth - bubbly opal
2069	35+03.78	fracture		blocky cal - botry'l opal - bladed cal - scepter cal o'gth
2070	35+23.63	fracture	calcite	(blocky cal) - short bladed cal - thin-bladed cal - scepter cal o'gth - opal coat
2071	35+45.4	fracture	calcite	fine grained blocky cal - coarser blocky cal - bladed cal - opal coat - cal o'gth
2072	35+57.2	fracture		bladed cal
2090	36+54.9	fracture	calcite	blocky cal - coarser blocky cal
2076	36+97.5	litho cavy		vapor phase - blocky cal - msv silica - (zeolite) - blocky cal - bladed cal
2080	37+60	fracture		(blocky cal) - bladed cal - (scepter cal o'gth)
2077 (A)	37+62.9	fracture		blocky cal - msv silica ± fluorite - bladed cal - scepter cal o'gth

Appendix 1. Paragenetic sequences of secondary mineral occurrences within the Exploratory Studies Facility (ESF), Yucca Mountain, Nevada (Continued)

Sample #	ESF Location*	Type	Basal Dissolution	
2077 (B)	37+62.9	fracture		blocky cal - msv silica - bladed cal - scepter cal o'gth - bubbly opal - cal o'gth
2078	37+67	litho cavy	calcite	vapor phase - blocky cal - msv silica - bladed cal - bubbly opal - scepter cal o'gth - opal coat + tiny bubbly opal
2079 (A)	38+17.2	litho cavy		msv silica - vapor phase - blocky cal
2079 (B)	38+17.2	litho cavy	calcite	msv silica - vapor phase - blocky cal - bladed cal - scepter cal o'gth
2079 (C)	38+17.2	litho cavy	calcite	vapor phase - blocky cal w/ scattered msv silica - bladed cal - scepter cal o'gth - bubbly opal - cal o'gths - opal coat - bubbly opal - cal o'gth
2081	38+61	litho cavy		vapor phase - blocky cal - coarser blocky cal + fluorite - bubbly opal - cal o'gth - coat to fine bubbly opal - cal o'gth
2083	38+64.0	fracture		blocky cal - bladed cal
2082	38+68.8	litho cavy		vapor phase + msv silica - blocky cal - coarser blocky cal + fluorite - coat to bubbly opal - cal o'gth
2084 (A)	38+87.8	litho cavy	calcite	vapor phase - blocky cal - bladed cal - scepter cal o'gth - coat to bubbly opal - (cal o'gth)
2084 (B)	38+87.8	fracture		blocky to bladed cal - msv silica
2085	39+38.7	litho cavy	calcite	vapor phase + msv silica - fluorite - blocky cal - bladed cal - scepter cal - bubbly opal - cal o'gth - (opal coat)
2086	39+44.0	fracture gouge		multi-stage blocky cal
2087	39+50.7	litho cavy		vapor phase - blocky cal - bladed cal - bubbly opal - bladed cal \pm cal o'gth - bubbly opal coat
2088	39+61	fracture	calcite	blocky cal - msv silica - blocky cal
2089 (A)	39+91.4	litho cavy	calcite	vapor phase + msv silica - blocky cal - bladed cal - scepter cal o'gth - opal coat
2089 (B)	39+91.4	litho cavy	calcite	vapor phase + msv silica - blocky cal - bladed cal - scepter cal o'gths - coat to bubbly opal - cal o'gth

GLOSSARY OF TERMS AND ABBREVIATIONS USED IN APPENDIX AND TEXT

Basal Dissolution:	"calcite" or "silica" in this column indicates possible later corrosion at the tuff-mineralization contact
Paragenesis:	the interpreted sequence of mineral deposition from first to last
litho cavy:	lithophysal cavity (identified by presence of vapor-phase minerals)
fracture:	secondary mineralization on fracture surface (does not preclude presence of vapor-phase minerals)
vapor phase:	refers to minerals, most commonly tridymite and hematite, precipitated during post-eruption cooling
msv silica:	massive silica - typically preceding calcite/late opal; a mixture of chalcedony, quartz, and possibly opal
freegrowth:	a mineralization stage in which the mineral form or crystal faces indicate growth into open space; may be covered by later precipitation
calcite (cal):	
- anhedral:	rare early stage of tightly intergrown calcite grains
- blocky:	a freegrowth stage of equant to thick tabular calcite crystals
- bladed:	a freegrowth stage of tabular calcite, typically tall and broad, but very thin
- scepter o'gth:	calcite overgrowth on blades resulting in blade tops much thicker than their bases
- o'gth:	minor deposition of later calcite on earlier calcite crystals
opal:	
- coat:	thin, laminar coating of opal, typically on crystal faces of calcite
- bubbly:	scattered grains or aggregates of grains of opal with a soap-bubble-like form
- botry'l:	botryoidal denotes a thick occurrence of laminar opal with a hummocky, rounded surface
fluorite:	a calcium-fluoride mineral that occurs locally as an accessory phase
zeolite:	any zeolite mineral within the mineralization sequence, except as the earliest fracture coating
():	indicates some uncertainty in either paragenetic position, mineral identification, or feature identification
* - Tunnel distance indicated in meters x 100, measured from portal	

Appendix 2. Calcite delta carbon-13 and delta oxygen-18 values from secondary mineral occurrences within the Exploratory Studies Facility (ESF) and drill holes near Yucca Mountain, Nevada

Sample #	Locality	Depth/Distance: m*	$\delta^{13}\text{-C}$ PDB	$\delta^{18}\text{-O}$ SMOW
HD-1837 b	ESF	98.80	-4.0	19.1
HD-1837 d	ESF	98.80	-4.1	19.9
HD-1837 c	ESF	98.80	-5.2	19.1
HD-1837 d	ESF	98.80	-4.1	20.0
HD-1837 a	ESF	98.90	-3.4	19.7
HD-1836 Aa	ESF	109.05	-4.4	19.7
HD-1836 Ba	ESF	109.05	-5.9	18.9
HD-1850 a	ESF	111.17	-5.7	19.1
HD-1850 b	ESF	111.17	-3.3	19.7
HD-1850 c	ESF	111.17	-1.4	19.3
HD-1838 a	ESF	111.55	-6.7	19.0
HD-1838 b	ESF	111.55	-3.1	19.5
HD-1838 b	ESF	111.55	-3.2	19.6
HD-1852 a	ESF	149.47	-6.2	19.5
HD-1852 b	ESF	149.47	-3.0	17.6
HD-1852 a	ESF	149.47	-6.2	19.2
HD-1849 a	ESF	161.90	-1.1	12.8
HD-1919 sa	ESF	168.20	-4.5	18.4
HD-1927 sa	ESF	168.20	-6.1	19.4
HD-1933 sa	ESF	168.20	-5.0	18.4
HD-1933 sb	ESF	168.20	-6.3	19.5
HD-1839 a	ESF	288.90	-6.6	18.8
HD-1841 a	ESF	301.80	-2.6	20.6
HD-1840 a	ESF	324.49	-5.2	20.5
HD-1840 b	ESF	324.49	-5.3	20.1
HD-1948 sa	ESF	336.79	-5.5	19.4
HD-1848 b	ESF	358.95	-5.2	20.2
HD-1844 a	ESF	360.20	-5.3	20.0
HD-1843 a	ESF	371.00	-5.5	19.6
HD-1847 a	ESF	375.19	-5.5	19.9
HD-1847 b	ESF	375.19	-5.2	20.5
HD-1875 a	ESF	382.82	-5.2	20.3
HD-1880 a	ESF	412.40	-5.1	19.9
HD-1937 sa	ESF	444.60	-5.9	19.9
HD-1879 a	ESF	454.04	-5.3	20.5
HD-1881 a	ESF	465.45	-5.9	20.2
HD-1881 a	ESF	465.45	-6.0	20.1
HD-1877 b	ESF	473.40	-4.3	19.4
HD-1877 a	ESF	473.40	2.5	11.6

Appendix 2. Calcite delta carbon-13 and delta oxygen-18 values from secondary mineral occurrences within the Exploratory Studies Facility (ESF) and drill holes near Yucca Mountain, Nevada (Continued)

Sample #	Locality	Depth/Distance: m*	$\delta^{13}\text{-C PDB}$	$\delta^{18}\text{-O SMOW}$
HD-1882 b	ESF	473.40	-5.6	19.9
HD-1883 b	ESF	473.40	-0.2	16.4
HD-1878 a	ESF	483.05	-6.1	20.0
HD-1878 b	ESF	483.05	-5.4	19.9
HD-1940 sa	ESF	509.09	-5.7	20.0
HD-1940 sb	ESF	509.09	-5.9	20.2
HD-1945 sa	ESF	513.20	-4.8	19.7
HD-1945 sb	ESF	513.20	-5.0	20.1
HD-1873 a	ESF	529.40	-6.0	20.3
HD-1873 b	ESF	529.40	-5.8	20.1
HD-1941 sa	ESF	529.40	-2.1	20.3
HD-1865 a	ESF	531.25	-3.5	20.2
HD-1934 sa	ESF	532.49	-4.5	19.3
HD-1934 sb	ESF	532.49	-4.9	19.9
HD-1866 a	ESF	556.95	-6.5	19.9
HD-1944 sa	ESF	556.95	-6.2	19.0
HD-1869 a	ESF	557.09	-6.2	19.6
HD-1876 a	ESF	577.03	-6.4	19.4
HD-1868 a	ESF	579.15	-6.4	18.8
HD-1868 b	ESF	579.15	-6.2	19.4
HD-1867 a	ESF	584.75	-5.5	18.6
HD-1870 a	ESF	588.15	-5.5	18.2
HD-1870 b	ESF	588.15	-6.6	19.0
HD-1872 a	ESF	640.20	-6.2	18.6
HD-1942 sa	ESF	652.70	-3.4	18.8
HD-1942 sb	ESF	652.70	-6.7	18.8
HD-1935 sa	ESF	658.75	-6.1	18.7
HD-1952 sa	ESF	803.80	-6.2	18.4
HD-1939 sa	ESF	818.20	-6.8	18.7
HD-1939 sb	ESF	818.20	-6.8	18.6
HD-1922 sb	ESF	822.68	-6.5	18.8
HD-1918 sa	ESF	988.97	-6.8	18.3
HD-1923 sa	ESF	1008.00	-9.0	18.6
HD-1932 sc	ESF	1090.30	-0.2	14.3
HD-1931 sa	ESF	1114.75	-4.6	18.1
HD-1929 sa	ESF	1147.00	-5.9	18.2
HD-1938 sa	ESF	1212.05	-0.2	18.2
HD-2021 sa	ESF	1221.83	-6.2	17.7
HD-2023 sa	ESF	1406.00	-0.6	14.8
HD-2001 sa	ESF	1420.00	-2.5	17.3

Appendix 2. Calcite delta carbon-13 and delta oxygen-18 values from secondary mineral occurrences within the Exploratory Studies Facility (ESF) and drill holes near Yucca Mountain, Nevada (Continued)

Sample #	Locality	Depth/Distance: m*	$\delta^{13}\text{-C}$ PDB	$\delta^{18}\text{-O}$ SMOW
HD-2001 sb	ESF	1420.00	6.3	12.4
HD-2025 sa	ESF	1455.00	6.9	13.0
HD-2025 sb	ESF	1455.00	-3.7	18.2
HD-2026 sa	ESF	1472.53	-6.0	19.2
HD-2027 sa	ESF	1479.55	-2.0	18.1
HD-2028 sb	ESF	1505.25	-4.7	18.2
HD-2028 sa	ESF	1505.25	2.9	14.4
HD-2029 sa	ESF	1533.25	4.6	12.6
HD-2029 sb	ESF	1533.25	-4.6	18.3
HD-2030 sa	ESF	1568.58	0.2	16.2
HD-2030 sb	ESF	1568.58	3.6	15.1
HD-2002 sb	ESF	1599.95	4.8	14.6
HD-2002 sc	ESF	1599.95	-5.7	17.7
HD-2002 sa	ESF	1599.95	4.1	14.7
HD-2003 sa	ESF	1612.38	6.2	11.5
HD-2003 sb	ESF	1612.38	7.6	13.5
HD-2003 sc	ESF	1612.38	-6.2	17.5
HD-2004 sc	ESF	1646.60	1.9	15.6
HD-2004 sb	ESF	1646.60	8.4	13.0
HD-2004 sa	ESF	1646.60	4.5	13.3
HD-2004 sb	ESF	1646.60	8.3	12.9
HD-2032 sa	ESF	1670.10	5.4	10.5
HD-2032 sb	ESF	1670.10	5.8	12.3
HD-2032 sc	ESF	1670.10	2.4	16.1
HD-2005 sa	ESF	1710.95	-6.3	17.8
HD-2005 sa	ESF	1710.95	-6.3	17.7
HD-2006 sa	ESF	1900.00	-0.6	15.0
HD-2006 sb	ESF	1900.00	0.0	13.9
HD-2006 sc	ESF	1900.00	-6.2	17.7
HD-2075 sa	ESF	1975.00	-5.4	17.5
HD-2075 sb	ESF	1975.00	-4.6	13.6
HD-2075 sc	ESF	1975.00	-6.5	17.1
HD-2007 1sb	ESF	2213.00	-5.8	16.9
HD-2007 1sc	ESF	2213.00	-6.1	15.9
HD-2007 2sa	ESF	2213.00	-7.0	15.9
HD-2007 1sb	ESF	2213.00	-5.6	17.1
HD-2007 2sb	ESF	2213.00	-7.2	16.6
HD-2007 1sa	ESF	2213.00	-6.1	16.0
HD-2007 2sa	ESF	2213.00	-7.1	16.0
HD-2008 sa	ESF	2272.00	-4.2	17.2

Appendix 2. Calcite delta carbon-13 and delta oxygen-18 values from secondary mineral occurrences within the Exploratory Studies Facility (ESF) and drill holes near Yucca Mountain, Nevada (Continued)

Sample #	Locality	Depth/Distance: m*	$\delta^{13}\text{-C PDB}$	$\delta^{18}\text{-O SMOW}$
HD-2008 sb	ESF	2272.00	-6.7	17.3
HD-2008 sa	ESF	2272.00	-4.7	15.4
HD-2020 sub1 sa	ESF	2439.58	-0.7	16.8
HD-2020 sub2 sb	ESF	2439.58	-1.9	16.3
HD-2020 sub2 sc	ESF	2439.58	-1.8	17.1
HD-2020 sub3 sd	ESF	2439.58	-2.7	16.5
HD-2020 sub1 sa	ESF	2439.58	-0.9	16.7
HD-2009 sa	ESF	2443.50	-3.8	17.0
HD-2009 sb	ESF	2443.50	-6.7	18.0
HD-2010 sa	ESF	2468.20	-6.9	18.0
HD-2010 sb	ESF	2468.20	-5.7	18.4
HD-2011 sa	ESF	2568.00	-1.2	16.7
HD-2011 sb	ESF	2568.00	-5.7	18.1
HD-2012 sa	ESF	2576.70	-4.1	17.4
HD-2012 sb	ESF	2576.70	-6.3	18.4
HD-2012 sc	ESF	2576.70	-5.8	17.4
HD-2013 sa	ESF	2678.58	4.8	14.5
HD-2013 sb	ESF	2678.58	-4.1	16.7
HD-2014 sa	ESF	2688.00	-2.1	16.3
HD-2015 sb	ESF	2695.00	-5.7	16.8
HD-2016 sa	ESF	2718.38	-2.4	16.1
HD-2016 sb	ESF	2718.38	-2.3	15.9
HD-2016 sc	ESF	2718.38	-5.8	16.7
HD-2017 sa	ESF	2724.00	4.2	14.1
HD-2017 sb	ESF	2724.00	-2.0	15.3
HD-2017 sc	ESF	2724.00	0.6	15.8
HD-2017 sd	ESF	2724.00	-7.4	17.2
HD-2017 sb	ESF	2724.00	0.7	15.6
HD-2018 sa	ESF	2750.65	4.2	13.5
HD-2018 sb	ESF	2750.65	-7.3	16.9
HD-2019 sc	ESF	2880.00	1.8	15.1
HD-2019 sd	ESF	2880.00	-2.6	13.8
HD-2019 sb	ESF	2880.00	6.7	13.5
HD-2019 sc	ESF	2880.00	-3.4	15.3
HD-2019 sf	ESF	2880.00	-7.2	17.2
HD-2019 sa	ESF	2881.00	-5.3	16.6
HD-2019 sg	ESF	2881.00	4.9	13.2
HD-2019 sh	ESF	2881.00	-6.9	16.6
HD-2054 sc	ESF	2881.60	4.2	14.7
HD-2054 sd	ESF	2881.60	1.6	15.2

Appendix 2. Calcite delta carbon-13 and delta oxygen-18 values from secondary mineral occurrences within the Exploratory Studies Facility (ESF) and drill holes near Yucca Mountain, Nevada (Continued)

Sample #	Locality	Depth/Distance: m*	$\delta^{13}\text{-C}$ PDB	$\delta^{18}\text{-O}$ SMOW
HD-2054 sc	ESF	2881.60	-6.9	16.7
HD-2054 sa	ESF	2881.60	4.9	14.2
HD-2054 sb	ESF	2881.60	4.2	13.7
HD-2055 sb	ESF	2911.20	-2.0	15.7
HD-2055 sc	ESF	2911.20	-5.6	16.9
HD-2055 se	ESF	2911.20	-6.7	17.8
HD-2055 sa	ESF	2911.20	7.7	14.0
HD-2055 sd	ESF	2911.20	-6.9	17.6
HD-2056 sa	ESF	2922.90	-6.2	17.0
HD-2056 sc	ESF	2922.90	-1.5	16.4
HD-2056 sb	ESF	2922.90	-3.1	16.8
HD-2056 sd	ESF	2922.90	-2.5	16.4
HD-2056 se	ESF	2922.90	-6.8	17.4
HD-2057 sa	ESF	2962.20	-7.3	17.3
HD-2057 sb	ESF	2962.20	-7.3	17.3
HD-2057 sc	ESF	2962.20	-7.4	17.4
HD-2057 se	ESF	2962.20	5.0	15.6
HD-2057 sf	ESF	2962.20	-7.3	17.5
HD-2057 sg	ESF	2962.20	6.8	14.0
HD-2057 sh	ESF	2962.20	0.4	16.7
HD-2057 si	ESF	2962.20	0.8	17.4
HD-2057 sj	ESF	2962.20	-7.8	17.2
HD-2058 sc	ESF	2979.98	-6.8	17.5
HD-2058 sa	ESF	2979.98	0.4	16.5
HD-2058 sb	ESF	2979.98	-0.4	16.9
HD-2058 sd	ESF	2979.98	-7.7	16.8
HD-2059 sc	ESF	3017.78	-7.2	16.7
HD-2059 se	ESF	3017.78	-7.3	16.8
HD-2059 sa	ESF	3017.78	-8.0	16.9
HD-2059 sb	ESF	3017.78	-8.1	16.7
HD-2059 sf	ESF	3017.78	3.5	14.9
HD-2059 sk	ESF	3017.78	-6.0	16.6
HD-2059 sl	ESF	3017.78	-7.2	16.9
HD-2059 sj	ESF	3017.78	-0.6	15.8
HD-2059 si	ESF	3017.78	1.7	15.1
HD-2059 sj	ESF	3017.78	-0.5	15.6
HD-2059 sl	ESF	3017.78	-7.2	16.8
HD-2060 sb	ESF	3026.58	-5.1	16.3
HD-2060 sc	ESF	3026.58	-7.1	16.8
HD-2060 sa	ESF	3026.58	4.4	14.1

Appendix 2. Calcite delta carbon-13 and delta oxygen-18 values from secondary mineral occurrences within the Exploratory Studies Facility (ESF) and drill holes near Yucca Mountain, Nevada (Continued)

Sample #	Locality	Depth/Distance: m*	$\delta^{13}\text{-C}$ PDB	$\delta^{18}\text{-O}$ SMOW
HD-2074 sb	ESF	3050.70	5.9	14.6
HD-2074 sc	ESF	3050.70	0.8	14.6
HD-2074 sd	ESF	3050.70	-3.2	14.5
HD-2074 se	ESF	3050.70	-7.3	17.0
HD-2061 sc	ESF	3057.68	6.5	14.6
HD-2061 sd	ESF	3057.68	-3.1	15.7
HD-2061 se	ESF	3057.68	-1.2	14.8
HD-2061 sf	ESF	3057.68	-6.4	16.9
HD-2061 sg	ESF	3057.68	-7.2	16.9
HD-2061 sb	ESF	3057.68	2.0	14.9
HD-2061 sb	ESF	3057.68	2.5	14.8
HD-2073 sb	ESF	3103.00	-2.2	14.8
HD-2073 sc	ESF	3103.00	-6.6	17.5
HD-2073 sd	ESF	3103.00	-7.5	17.3
HD-2073 se	ESF	3103.00	-7.5	16.9
HD-2073 sa	ESF	3103.00	6.2	14.6
HD-2073 se	ESF	3103.00	-7.6	16.9
HD-2073 se	ESF	3103.00	-6.8	17.1
HD-2062 sa	ESF	3107.40	-7.1	17.5
HD-2062 sb	ESF	3107.40	-0.3	16.1
HD-2062 sc	ESF	3107.40	-6.8	17.3
HD-2062 sd	ESF	3107.40	-7.6	17.2
HD-2063 sa	ESF	3116.10	0.0	16.7
HD-2063 sb	ESF	3116.10	-5.8	17.2
HD-2064 sa	ESF	3195.70	1.9	15.5
HD-2065 sa	ESF	3316.20	7.4	15.0
HD-2065 sb	ESF	3316.20	4.9	15.2
HD-2065 sc	ESF	3316.20	6.3	14.7
HD-2065 sd	ESF	3316.20	6.7	14.5
HD-2065 sf	ESF	3316.20	7.4	14.7
HD-2065 sg	ESF	3316.20	7.2	14.7
HD-2065 sh	ESF	3316.20	6.3	14.8
HD-2065 si	ESF	3316.20	5.0	15.4
HD-2065 sj	ESF	3316.20	6.8	14.6
HD-2065 sk	ESF	3316.20	6.6	14.3
HD-2065 sl	ESF	3316.20	4.1	15.2
HD-2065 sn	ESF	3316.20	-6.5	17.5
HD-2065 sc	ESF	3316.20	6.4	14.5
HD-2065 se	ESF	3316.20	6.8	14.4
HD-2066 sa	ESF	3395.78	-1.6	17.4

Appendix 2. Calcite delta carbon-13 and delta oxygen-18 values from secondary mineral occurrences within the Exploratory Studies Facility (ESF) and drill holes near Yucca Mountain, Nevada (Continued)

Sample #	Locality	Depth/Distance: m*	$\delta^{13}\text{-C}$ PDB	$\delta^{18}\text{-O}$ SMOW
HD-2066 sb	ESF	3395.78	-2.1	17.5
HD-2066 sc	ESF	3395.78	-5.7	18.3
HD-2066 sd	ESF	3395.78	-7.0	17.7
HD-2066 se	ESF	3395.78	-6.4	18.5
HD-2067 sb	ESF	3428.18	-0.9	16.5
HD-2067 sc	ESF	3428.18	-5.3	17.1
HD-2067 sd	ESF	3428.18	1.0	15.9
HD-2067 sa	ESF	3428.18	-0.6	16.9
HD-2068 sa	ESF	3486.48	0.1	16.0
HD-2068 sb	ESF	3486.48	-5.8	17.3
HD-2069 sb	ESF	3503.78	-3.3	16.1
HD-2069 sc	ESF	3503.78	-6.5	16.9
HD-2069 se	ESF	3503.78	-6.4	17.1
HD-2069 sa	ESF	3503.78	2.3	15.3
HD-2070 sa	ESF	3523.63	-1.5	15.8
HD-2070 sb	ESF	3523.63	-6.4	17.1
HD-2071 sa	ESF	3545.40	1.5	15.1
HD-2071 sb	ESF	3545.40	5.3	14.8
HD-2071 sc	ESF	3545.40	-6.4	17.2
HD-2071 sd	ESF	3545.40	-5.5	17.3
HD-2071 se	ESF	3545.40	2.0	15.0
HD-2072 sa	ESF	3557.20	3.4	14.7
HD-2076 sa	ESF	3697.50	-1.4	15.7
HD-2076 sb	ESF	3697.50	-2.5	15.5
HD-2076 sc	ESF	3697.50	-6.1	16.5
HD-2077 Asa	ESF	3762.90	1.8	15.4
HD-2077 Asb	ESF	3762.90	-6.4	17.6
HD-2077 Bsc	ESF	3762.90	4.3	14.5
HD-2077 Bsd	ESF	3762.90	-1.5	15.9
HD-2077 Bse	ESF	3762.90	-7.7	17.5
HD-2078 sb	ESF	3767.00	-0.6	15.6
HD-2078 sc	ESF	3767.00	-0.8	15.5
HD-2078 sd	ESF	3767.00	-6.5	17.6
HD-2078 sa	ESF	3767.00	2.4	15.6
HD-2079 Asa	ESF	3817.20	-1.2	16.4
HD-2079 Bsb	ESF	3817.20	3.2	15.7
HD-2079 Bsc	ESF	3817.20	-3.3	17.0
HD-2079 Bsd	ESF	3817.20	-6.0	17.6
HD-2079 Cse	ESF	3817.20	1.5	16.2
HD-2079 Csf	ESF	3817.20	-0.1	16.4

Appendix 2. Calcite delta carbon-13 and delta oxygen-18 values from secondary mineral occurrences within the Exploratory Studies Facility (ESF) and drill holes near Yucca Mountain, Nevada (Continued)

Sample #	Locality	Depth/Distance: m*	$\delta^{13}\text{-C PDB}$	$\delta^{18}\text{-O SMOW}$
HD-2079 Csg	ESF	3817.20	-7.0	18.0
HD-2079 Csh	ESF	3817.20	-7.2	18.0
HD-2081 sc	ESF	3861.00	-7.0	17.5
HD-2081 sa	ESF	3861.00	2.8	16.4
HD-2081 sb	ESF	3861.00	-0.5	16.9
HD-2083 sa	ESF	3864.00	-0.6	16.5
HD-2083 sb	ESF	3864.00	2.8	15.7
HD-2083 sc	ESF	3864.00	3.6	15.3
HD-2083 sd	ESF	3864.00	-5.4	16.9
HD-2082 sb	ESF	3868.80	2.0	15.3
HD-2084 Asa	ESF	3887.80	0.3	15.5
HD-2084 Asb	ESF	3887.80	-7.0	17.0
HD-2084 Asb	ESF	3887.80	-7.1	17.0
HD-2084 Bsa	ESF	3887.80	1.8	15.9
HD-2084 Bsb	ESF	3887.80	-3.3	17.6
HD-2085 sa	ESF	3938.70	1.2	15.7
HD-2085 sb	ESF	3938.70	0.9	15.7
HD-2086 sa	ESF	3944.00	5.1	14.7
HD-2086 sb	ESF	3944.00	-3.1	17.2
HD-2086 sc	ESF	3944.00	-5.8	17.5
HD-2086 sc	ESF	3944.00	-6.0	17.4
HD-2087 sb	ESF	3950.70	-5.8	17.5
HD-2087 sa	ESF	3950.70	-2.4	16.9
HD-2088 sa	ESF	3961.00	4.4	14.6
HD-2088 sb	ESF	3961.00	3.4	14.9
HD-2088 sc	ESF	3961.00	4.7	14.5
HD-2089 Asa	ESF	3991.40	-0.1	15.7
HD-2089 Asa	ESF	3991.40	-0.5	15.9
HD-2089 Asb	ESF	3991.40	-5.5	17.3
HD-2089 Bsa	ESF	3991.40	-3.5	16.5
HD-2089 Bsb	ESF	3991.40	-5.8	17.3
HD-769 a	UE-25 A-7	47.70	-7.0	18.6
HD-776 a	UE-25 A-7	92.90	-5.1	17.7
HD-777 a	UE-25 A-7	94.80	6.2	14.8
HD-778 a	UE-25 A-7	95.80	-6.1	17.7
HD-779 a	UE-25 A-7	97.80	-6.7	17.8
HD-780 a	UE-25 A-7	102.90	-6.2	17.8
HD-780 c	UE-25 A-7	102.90	-5.6	16.9
HD-780 b	UE-25 A-7	102.90	-5.2	16.0
HD-781 a	UE-25 A-7	105.90	-4.1	16.5

Appendix 2. Calcite delta carbon-13 and delta oxygen-18 values from secondary mineral occurrences within the Exploratory Studies Facility (ESF) and drill holes near Yucca Mountain, Nevada (Continued)

Sample #	Locality	Depth/Distance: m*	$\delta^{13}\text{-C}$ PDB	$\delta^{18}\text{-O}$ SMOW
HD-781 a	UE-25 A-7	105.90	-4.1	16.6
HD-783 a	UE-25 A-7	108.10	-6.5	17.8
HD-784 c	UE-25 A-7	113.00	-4.5	16.8
HD-785 a	UE-25 A-7	117.30	-4.5	17.8
HD-786 a	UE-25 A-7	124.40	-6.4	17.6
HD-787 a	UE-25 A-7	128.80	-6.9	17.8
HD-788 a	UE-25 A-7	131.00	-5.5	17.9
HD-790 a	UE-25 A-7	140.60	-5.5	14.8
HD-790 a	UE-25 A-7	140.60	-5.5	14.8
HD-791 a	UE-25 A-7	143.50	-6.3	17.9
HD-791 b	UE-25 A-7	143.50	1.0	14.0
HD-1833 a	UE-25 UZ-14	94.10	-4.8	15.2
HD-1834 a	UE-25 UZ-14	179.20	-6.0	16.2
HD-1835 a	UE-25 UZ-14	246.90	6.2	13.2
HD-1835 a	UE-25 UZ-14	246.90	6.8	13.0
HD-1644 a	USW SD-12	2.40	-7.1	20.0
HD-1650 a	USW SD-12	22.10	-6.0	19.7
HD-1651 a	USW SD-12	25.80	-6.2	19.8
HD-1652 a	USW SD-12	26.50	-5.1	19.5
HD-1653 a	USW SD-12	28.10	-6.1	19.8
HD-1654 b	USW SD-12	30.20	-4.3	19.4
HD-1654 a	USW SD-12	30.20	-3.6	19.3
HD-1655 a	USW SD-12	32.90	-7.3	20.0
HD-1655 b	USW SD-12	32.90	-4.5	19.6
HD-1655 c	USW SD-12	32.90	-6.4	19.3
HD-1655 a	USW SD-12	32.90	-7.3	19.9
HD-1656 a	USW SD-12	37.90	-5.4	20.0
HD-1656 b	USW SD-12	37.90	-6.3	19.1
HD-1657 a	USW SD-12	42.40	-5.8	19.1
HD-1658 a	USW SD-12	46.60	-8.0	19.0
HD-1659 a	USW SD-12	48.20	-7.4	19.4
HD-1660 a	USW SD-12	48.70	-5.6	19.0
HD-1661 a	USW SD-12	51.40	-5.0	19.9
HD-1662 a	USW SD-12	54.20	-5.4	19.5
HD-1663 a	USW SD-12	57.10	-2.4	18.7
HD-1664 a	USW SD-12	63.70	-3.9	19.1
HD-1665 a	USW SD-12	75.40	-7.3	18.9
HD-1666 a	USW SD-12	77.20	-7.0	19.3
HD-1667 a	USW SD-12	100.90	-5.2	18.7
HD-1667 b	USW SD-12	100.90	-5.3	18.6

Appendix 2. Calcite delta carbon-13 and delta oxygen-18 values from secondary mineral occurrences within the Exploratory Studies Facility (ESF) and drill holes near Yucca Mountain, Nevada (Continued)

Sample #	Locality	Depth/Distance: m*	$\delta^{13}\text{-C PDB}$	$\delta^{18}\text{-O SMOW}$
HD-1668 a	USW SD-12	132.60	-3.9	18.3
HD-1669 a	USW SD-12	141.80	-5.2	18.5
HD-1669 a	USW SD-12	141.80	-5.2	18.5
HD-1670 a	USW SD-12	146.70	-4.5	18.3
HD-1671 a	USW SD-12	149.30	-6.3	18.8
HD-1672 a	USW SD-12	160.60	-3.6	17.8
HD-1675 a	USW SD-12	223.30	-4.5	17.3
HD-1675 a	USW SD-12	223.30	-4.2	17.2
HD-1676 a	USW SD-12	223.50	-1.7	16.6
HD-1677 a	USW SD-12	282.50	-0.5	15.9
HD-1677 b	USW SD-12	282.50	-1.4	16.1
HD-1887 a	USW SD-7	17.40	-6.9	20.6
HD-1887 b	USW SD-7	17.40	-6.8	20.6
HD-1888 a	USW SD-7	34.00	-7.5	19.5
HD-1890 a	USW SD-7	49.80	-7.3	20.2
HD-1891 a	USW SD-7	94.40	-7.3	19.1
HD-1892 a	USW SD-7	95.20	-7.3	19.7
HD-1896 b	USW SD-7	301.90	-6.7	17.6
HD-747 b	USW VH-1	563.80	-0.5	25.5
HD-1250 a	USW VH-2	301.90	-1.2	17.9
HD-1250 a	USW VH-2	301.90	-1.2	18.2
HD-1251 a	USW VH-2	346.80	-1.1	16.3
HD-1251 b	USW VH-2	346.80	-1.6	16.0
HD-1252 a	USW VH-2	349.20	0.4	15.2
HD-1252 b	USW VH-2	349.20	-1.0	16.0
HD-728 b	USW VH-2	354.10	-0.7	17.0
HD-728 a	USW VH-2	354.10	1.0	13.8
HD-729 b	USW VH-2	356.30	-1.3	25.1
HD-730 a	USW VH-2	364.40	-2.9	14.8
HD-730 b	USW VH-2	364.40	-0.7	15.3
HD-731 c	USW VH-2	370.40	-1.5	15.3
HD-731 a	USW VH-2	370.40	-4.3	16.3
HD-731 b	USW VH-2	370.40	-4.3	17.0
HD-732 b	USW VH-2	372.30	-4.5	16.9
HD-732 d	USW VH-2	372.30	-2.1	14.5
HD-732 c	USW VH-2	372.30	-0.6	15.7
HD-732 a	USW VH-2	372.30	-8.0	16.6
HD-733 a	USW VH-2	375.80	-0.6	15.1
HD-733 a	USW VH-2	375.80	-0.5	15.1
HD-734 b	USW VH-2	379.00	-1.8	14.8

Appendix 2. Calcite delta carbon-13 and delta oxygen-18 values from secondary mineral occurrences within the Exploratory Studies Facility (ESF) and drill holes near Yucca Mountain, Nevada (Continued)

Sample #	Locality	Depth/Distance: m*	$\delta^{13}\text{-C}$ PDB	$\delta^{18}\text{-O}$ SMOW
HD-734 c	USW VH-2	379.00	-1.9	14.5
HD-734 a	USW VH-2	379.00	-3.9	16.4
HD-735 a	USW VH-2	385.80	-0.8	14.9
HD-736 a	USW VH-2	388.90	-4.0	16.4
HD-736 b	USW VH-2	388.90	-0.9	15.0
HD-742 a	USW VH-2	490.60	-4.1	14.8
HD-742 b	USW VH-2	490.60	-2.0	13.5
HD-743 b	USW VH-2	535.10	0.8	25.7
HD-743 a	USW VH-2	535.10	-0.2	23.6
HD-743 c	USW VH-2	535.10	0.4	24.8
HD-744 b	USW VH-2	538.30	0.3	20.4
HD-745 b	USW VH-2	550.50	-0.1	26.8
HD-745 a	USW VH-2	550.50	0.1	24.2
HD-747 a	USW VH-2	563.80	0.0	14.2
HD-748 b	USW VH-2	571.40	2.5	12.9
HD-748 a	USW VH-2	571.40	3.1	12.8
HD-748 c	USW VH-2	571.40	1.3	19.2
HD-749 b	USW VH-2	581.00	2.8	12.5
HD-749 a	USW VH-2	581.00	2.6	12.9
HD-749 c	USW VH-2	581.00	0.9	18.8
HD-749 c	USW VH-2	581.00	0.9	18.7
HD-750 b	USW VH-2	595.20	0.9	12.7
HD-750 a	USW VH-2	595.20	1.4	15.5
HD-750 d	USW VH-2	595.20	0.0	20.5
HD-759 a	USW VH-2	854.30	1.5	4.4
HD-759 b	USW VH-2	854.30	-1.9	13.0
HD-760 a	USW VH-2	865.30	1.4	5.7
HD-760 b	USW VH-2	865.30	-0.6	9.5
HD-761 b	USW VH-2	871.50	0.9	7.2
HD-761 a	USW VH-2	871.50	-1.9	11.6
HD-761 b	USW VH-2	871.50	0.9	7.2
HD-763 a	USW VH-2	874.60	-2.2	13.0
HD-763 b	USW VH-2	874.60	0.3	7.6
HD-764 a	USW VH-2	897.50	0.5	8.3

*-Depth in borehole or distance from ESF portal (in meters)

PDB-Pee Dee Belemnite standard

SMOW-Standard Mean Ocean Water standard

Appendix 3. Secondary silica and calcite delta oxygen-18 values from the Exploratory Studies Facility (ESF), drill holes, and outcrop samples obtained near Yucca Mountain, Nevada, and from the Bullfrog Mine.

Sample	Lab	Locality	Depth (ft)	Tuff Member	$\delta^{18}\text{-O}$ SMOW for silica	$\delta^{18}\text{-O}$ SMOW for calcite
HD-306c opal	ASU	UE-25 a#1	253	Tiva Canyon	18.6	16.9
HD-351b opal	ASU	USW G-2	92.2	Tiva Canyon	26.6	20.7
HD-355a opal	ASU	USW G-2	236.7	Tiva Canyon	20.5	17.9
HD-356a opal	ASU	USW G-2	240.7	Tiva Canyon	21.7	19.0
HD-358a opal	ASU	USW G-2	257.8	Yucca Mtn	24.1	17.4
HD-362a opal	ASU	USW G-2	280.2	Yucca Mtn	21.2	18.7
HD-929a opal	ASU	UE-25 a#5	92.2	Tiva Canyon	23.3	17.9
HD-926a opal	ASU	UE-25 a#5	85.2	Tiva Canyon	21.9	17.7
HD-700a opal	ASU	USW G-4	74.2	Tiva Canyon	24.1	no cal
349,P2 Cut 1	ASU	Trench 14		pedogenic	22.6	20.0
349,P2 Cut 2*	ASU	Trench 14		pedogenic	27.6	20.0
T-14 grab, Cut 1	ASU	Trench 14		pedogenic	26.1	20.0
T-14 grab, Cut 2*	ASU	Trench 14		pedogenic	24.0	20.0
7, P3, Cut 1	ASU	Trench 14		pedogenic	22.8	20.0
7,P3, Cut 2*	ASU	Trench 14		pedogenic	30.9	20.0
LANL 49, P1, Cut 2*	ASU	Trench 14		pedogenic	22.5	20.0
LANL 49, P1, Cut 1	ASU	Trench 14		pedogenic	31.3	20.0
HD-577b qtz	USGS	USW G-2	4116.4	un-named lava	5.9	15.8
HD-590b chal	USGS	USW G-2	5635.8	un-named lava	10.2	5.8
HD-406b tridy	USGS	USW GU-3	630		11.5	20.1
HD-304c qtz	USGS	UE-25 a#1	780.6	Topopah Spg	11.3	17.2
HD-307b qtz	USGS	UE-25 a#1	845.6	Topopah Spg	17.9	16.4
HD-308a tridy	USGS	UE-25 a#1	898.1	Topopah Spg	12.5	no cal
HD-1497b qtz	USGS	UE-25 NRG#2	187		20.8	19.8
HD-1500a qtz	USGS	UE-25 NRG#2	210.5		8.6	no cal
HD-939-1-c qtz	USGS	Bullfrog Mine	958 bench		5.6	5.8
HD-940c opal	USGS	Bullfrog Mine	1024 bench		24.8	19.2
HD-941f qtz	USGS	Bullfrog Mine	1042 bench		8.5	5.0
HD-941g opal	USGS	Bullfrog Mine	1042 bench		21.5	5.0
HD-1184c qtz	USGS	ESF			19.4	19.5
HD-1189c qtz	USGS	ESF-6			16.8	19.4
HD-1189d qtz	USGS	ESF-6			14.1	19.4
HD-1191b qtz	USGS	ESF-8, bag 3			20.7	19.3
HD-1191c chal	USGS	ESF-8, bag 3			14.6	19.3
HD-270b qtz	USGS	USW G-3	4803		6.9	7.5
HD-1186f qtz	USGS	ESF-3			19.0	17.1
HD-1186g chal	USGS	ESF-3			7.9	17.1
HD-1186h qtz	USGS	ESF-3			20.2	17.1

Appendix 3. Secondary silica and calcite delta oxygen-18 values from the Exploratory Studies Facility (ESF), drill holes, and outcrop samples obtained near Yucca Mountain, Nevada, and from the Bullfrog Mine. (Continued)

Sample	Lab	Locality	Depth (ft)	Tuff Member	$\delta^{18}\text{O}$ SMOW for silica	$\delta^{18}\text{O}$ SMOW for calcite
HD-1563b opal	USGS	USW UZ-14	291.4		20.1	16.7
HD-1566b opal	USGS	USW UZ-14	310.1		23.4	17.2
HD-1568b opal	USGS	USW UZ-14	319.4		22.8	17.9
HD-1573b tridy	USGS	USW UZ-14	1043.6		14.2	14.8
HD-1584a chal	USGS	UE-25 NRG#3	253.1		8.4	no cal
HD-1667c opal	USGS	USW SD-12	331.1		24.0	18.7
HD-1678 opal	USGS	YM-2-SSL P2		Tiva Canyon	27.9	no cal
HD-1679a late opal	USGS	YF-4-SSL		Topopah Spg	25.7	no cal
HD-1679b msv chal	USGS	YF-4-SSL		Topopah Spg	17.3	no cal
HD-1679c msv chal	USGS	YF-4-SSL		Topopah Spg	10.3	no cal
HD-1679d milky opal	USGS	YF-4-SSL		Topopah Spg	18.5	no cal
HD-1679e milky opal	USGS	YF-4-SSL		Topopah Spg	18.3	no cal
HD-1679f early chal	USGS	YF-4-SSL		Topopah Spg	11.4	no cal
HD-1680c opal	USGS	NRST-1-SSL		Tiva Canyon	20.3	no cal
HD-803a tridy	USGS	UE25a #7	728.5		15.1	no cal
HD-1837e early chal	USGS	ESF 98.8		Tiva Canyon	13.9	19.1
HD-1838c young opal	USGS	ESF 111.55		Tiva Canyon	22.5	19.5
HD-1838d late opal	USGS	ESF 111.55		Tiva Canyon	23.0	19.0
HD-1839b surface opal	USGS	ESF 2+88.19		Tuff X	26.6	18.8
HD-1848c surface opal	USGS	ESF 358.95		Tiva Canyon	22.3	20.2
HD-1848d LN opal	USGS	ESF 358.95		Tiva Canyon	18.0	20.2
HD-1865b opal bubbles	USGS	ESF 5+31.25		Tiva Canyon	23.0	20.2
HD-1865c qtz	USGS	ESF 5+31.25		Tiva Canyon	21.2	20.2
HD-1865d LN opal rose	USGS	ESF 5+31.25		Tiva Canyon	22.4	20.2
HD-1865e LN young opal	USGS	ESF 5+31.25		Tiva Canyon	19.9	20.2
HD-1870c tridy	USGS	ESF 5+88.15		Tiva Canyon	13.5	18.6
HD-1875b opal	USGS	ESF 382.82		Tiva Canyon	22.8	20.3
HD-1875c qtz	USGS	ESF 382.82		Tiva Canyon	21.5	20.3
HD-1882a lithophysal qtz	USGS	ESF 4+73.4		Tiva Canyon	22.8	19.9
HD-1883a choq	USGS	ESF 4+73.4		Tiva Canyon	13.0	16.4
HD-1889a tridy	USGS	USW SD-7	132		8.8	no cal
HD-1893a tridy	USGS	USW SD-7	919.8		19.7	no cal
HD-1894a early tridy	USGS	USW SD-7	955.3		17.8	no cal
HD-1894b late qtz	USGS	USW SD-7	955.3		19.6	no cal
HD-1895a early tridy	USGS	USW SD-7	969.6		18.7	no cal
HD-1895b late qtz	USGS	USW SD-7	969.6		19.9	no cal
HD-1896a early qtz	USGS	USW SD-7	990.4		20.3	17.6
HD-1897a qtz	USGS	USW SD-7	1069.3		19.0	no cal
HD-1921a early chal	USGS	ESF 10+28.05		pre Pah Canyon	15.0	no cal
HD-1922a opal	USGS	ESF 8+22.68		Tiva Canyon	23.3	18.8

The distribution code for this report is UC-814.

Whelan and others—APPLICATIONS OF ISOTOPE GEOCHEMISTRY TO THE RECONSTRUCTION OF YUCCA MOUNTAIN, NEVADA,
PALEOHYDROLOGY—STATUS OF INVESTIGATIONS: JUNE 1996—USGS/OFR 98-83